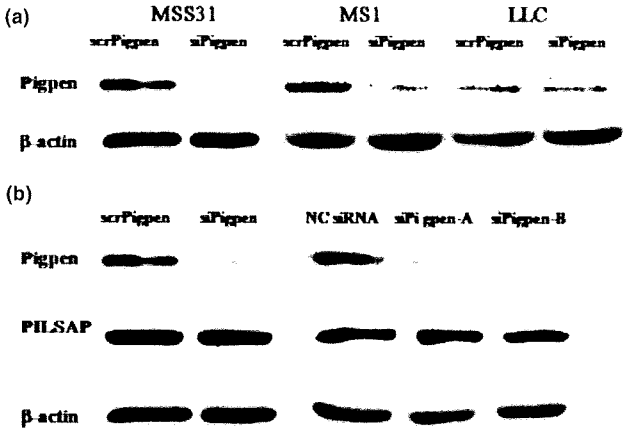

Fig. 2. Western blot of pigpen in scr- or siPigpen-transfected MSS31, MS1, and Lewis lung carcinoma (LLC) cells (a). Western blot of pigpen and PILSAP in MSS31 transfected with scr- or siPigpen, siPigpen-A, siPigpen-B, or nontargeting siRNA (NC siRNA) as a negative control for siPigpen-A and -B (b). Equal loading was confirmed by β-actin.

conjugated donkey antirabbit IgG (Invitrogen) in RB at RT for 1 h. Nuclei were stained with TO-PRO-3 (Invitrogen). Cells were washed with PBS at RT for 5 min twice between each steps. Images were photographed by a Zeiss LSM 510 confocal microscope system (Carl Zeiss, Oberkochen, Germany).

Inhibition of pigpen expression by siRNA. Control or siRNA oligonucleotides at a final concentration of 10 nM were transfected into MS1, MSS31, and LLC cells using Lipofectamine RNAiMAX Transfection Reagent (Invitrogen). The sequences of siPigpen and scrPigpen were as follows: 5′-GAACAGGAUAAUUCAGACATT-3′ and 5′-AAUCGAAUUAGCAGGAAACTT-3′, respectively. The sequences of the other set, siPigpen-A, siPigpen-B, and nontargeting control siRNA (NC siRNA) as a negative control for these two siRNAs were as follows: 5′-CAAACGACUAUACCCAACATT-3′, 5′-CAAUACCAUCUUCGUGCAATT-3′, and 5′-UCUUAAUCGCGUAUAAGGCTT-3′, respectively. The efficacy of siRNAs for pigpen was evaluated by mRNA (data not shown) and protein levels.

Western blotting. The protein extracts (20 μg) from MSS31, MS1, and LLC cells transfected with scr- or siPigpen for 24 h were applied to a western blot with 2 μg/mL anti-mPigpen Ab or anti-mPILSAP Ab. The signals were detected with ECL plus western blotting detection reagents and visualized using LAS1000. Equal loading was confirmed by blotting with anti-β-actin Ab (Sigma).

EC proliferation assay. At 24 h after transfection of scr- or siPigpen into MSS31 or LLC cells (2000 cells/well in a 96-well-plate), cells were incubated in 0.1% αMEM with or without 50 ng/mL VEGF (MSS31) or 1 or 10% DMEM for another 24 h. In some experiment, cells were transfected with scr- or siPigpen, NC siPigpen, siPigpen-A, or siPigpen-B on the day before an assay. MS1 or MSS31 cells (20 000 or 10 000/well, respectively) were inoculated in a 96-well-plate and incubated in 0.1% HG-DMEM or 0.1% αMEM. After 24-h incubation, the medium of MS1 was changed to 100 μL/well of 0.1%

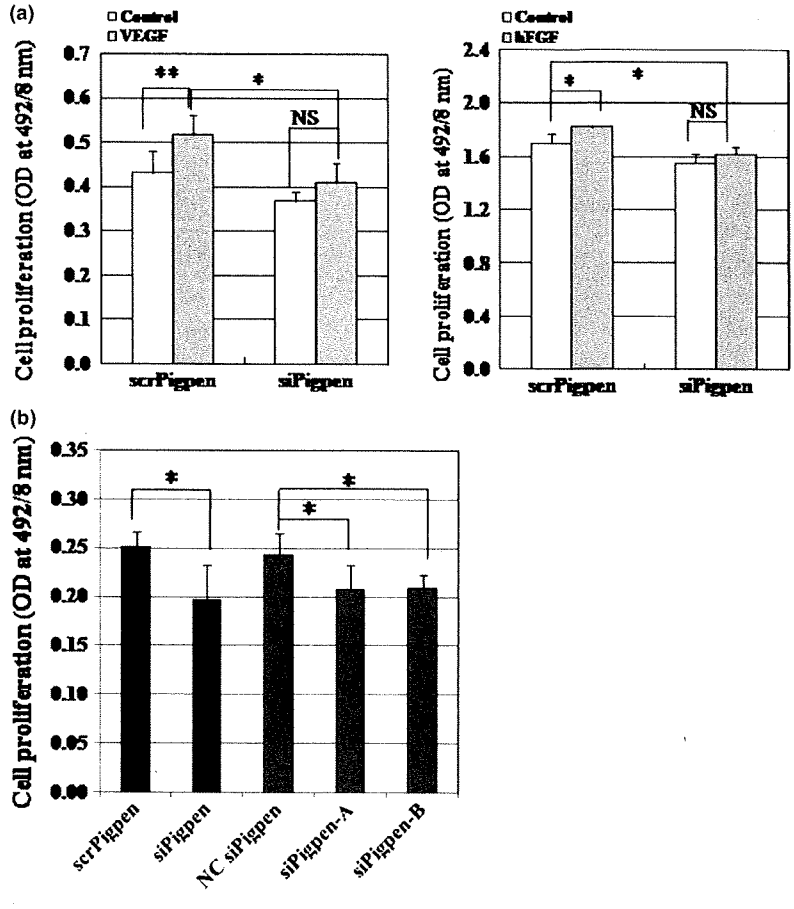

Fig. 3. (a) Endothelial cell (EC) proliferation assay of MSS31 (left) and MS1 (right) cells transfected with scr- or siPigpen. MSS31 cells were treated with or without 50 ng/mL vascular endothelial growth factor (VEGF) for 24 h ($n = 6$). MS1 cells were treated with or without 20 ng/mL basic fibroblast growth factor (bFGF) for 24 h ($n = 3$). (b) EC proliferation assay of MSS31 cells transfected with scr- or siPigpen, nontargeting control siRNA (NC siRNA), siPigpen-A, or siPigpen-B. ($n = 6$ for scr- or siPigpen and $n = 5$ for NC siRNA, siPigpen-A, or siPigpen-B). Bars indicate SDs. $^*P < 0.05$, $^{**}P < 0.01$.

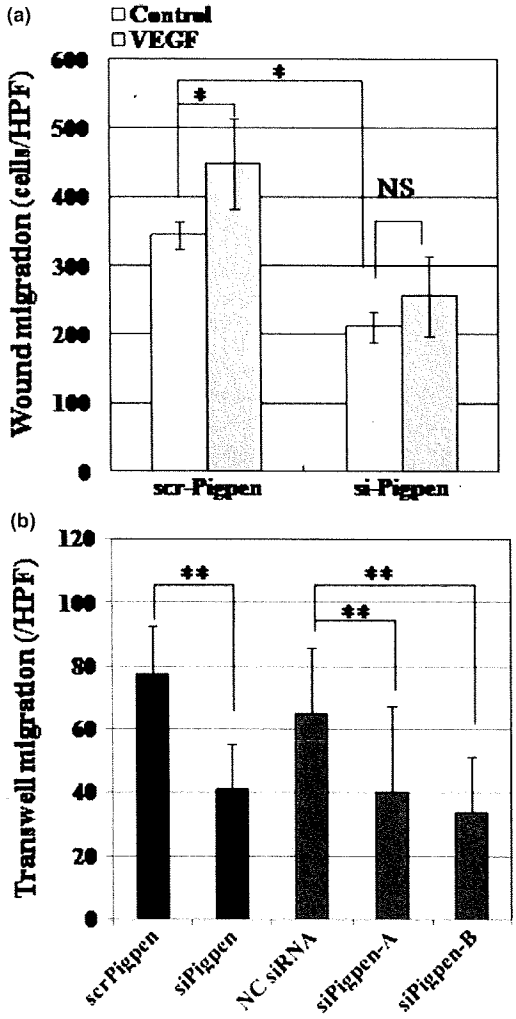

Fig. 4. (a) Wound migration assay of scr- or siPigpen-transfected MS1 cells with vehicle or 50 ng/mL vascular endothelial growth factor (VEGF) (n = 6). (b) Transwell migration assay of MSS31 cells transfected with scr- or siPigpen, nontargeting control siRNA (NC siRNA), siPigpen-A, or siPigpen-B (n = 12). Data indicate means and SDs. *P < 0.05, **P < 0.01.

HG-DMEM with or without 20 ng/mL bFGF and MS1 cells were incubated for an additional 24 h. MSS31 cells were incubated for 48 h. Cell numbers were analyzed with a Cell Titer 96 Aqueous Assay (Promega, Madison, WI, USA).

EC wound migration assay. At 10 h after transfection of scr- or siPigpen into MS1 cells, medium was changed to growth medium. After 14-h incubation, cells were replated into 12-well plates at a density of 200 000/well. The next day, confluent monolayers were wounded with a yellow tip, and cells were incubated in 0.1% HG-DMEM for an additional 24 h. Cells that had migrated into the denuded area were counted.

Transwell migration assay. MSS31 cells were transfected with scr- or siPigpen, NC siPigpen, siPigpen-A, or siPigpen-B. Next day cells were starved in 0.1% αMEM for 2 h and replated in 0.1% αMEM on a filter of 8-μm pore size in the upper insert of 24-well transwell chambers (Corning, Acton, MA, USA) at the density of 47 500 cells/95 μL/well. Six-hundred microliter of 0.1% αMEM with or without 20 ng/mL bFGF was added into the lower chamber. After 7-h incubation, unmigrated cells on the upper side of the filter were scraped off with a cotton swab

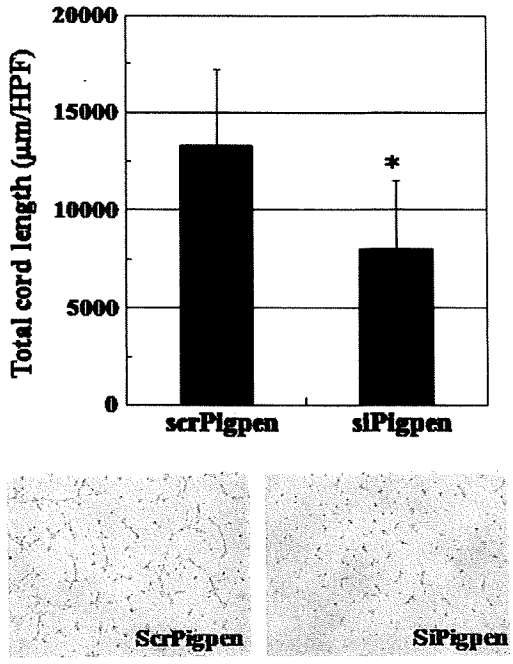

Fig. 5. Network formation of MS1 cells transfected with scr- or siPigpen. Data indicate means and SDs, n = 6. *P < 0.05. Repre sentative images are shown.

and the filters were fixed and stained with 0.1% crystal violet in 70% ethanol for 30 min. Migration was quantified by counting cells in randomly selected high power fields (HPF).

EC network formation assay. MS1 cells treated as described above were inoculated onto 96-well plates coated with growth factor-reduced Matrigel (GFR-Matrigel; BD Biosciences) at a density of 20 000 per well. Under these conditions, cells began to form tubes, and 4 h later, the tube length was measured with a BZ Analyzer (Keyence, Osaka, Japan).

Matrigel plug assay. GFR-Matrigel (500 μL) containing 100 ng/mL bFGF (BD Biosciences), 32 U/mL heparin, and 200 nM scr- or siPigpen was subcutaneously injected into 5-week-old male C57BL/6 mice. On day 6, Matrigel was removed for immunohistochemistry (IHC) of vascular endothelial (VE)-cadherin and hemoglobin (Hb) measurement. Hb content was measured using a hemoglobin B test (Wako, Osaka, Japan). The number of blood vessels positive for VE-cadherin was counted under a fluorescent microscope (Biozero BZ-8000, Keyence).

Syngenic tumor implantation model. A mixture of 150 μL GFR-Matrigel and 150 μL of Hanks' Balanced Salt Solution (HBSS) containing 500 000 LLC cells was subcutaneously injected into 5-week-old male C57BL/6 mice. On day 5, 100 pmol scr- or siPigpen was injected into the tumors. Every 3 days, the tumor volume was measured with calipers, and the injection of scr- or siPigpen was repeated. Tumor volume was estimated by using the formula of a (the major axis) × b (the minor axis)^2/2. On day 14, tumors were removed for IHC for CD31, and the length of CD31-positive tubes was measured with a BZ Analyzer (Keyence).

All protocols for experiments involving animals were approved by the Tokyo Medical and Dental University Bioethical and Animal Care Ethics Committees and conformed to the provisions of the Declaration of Helsinki in 1995 (as revised in Tokyo in 2004).

IHC analysis. Tissues from the Matrigel plug assay and the syngenic tumor implantation model were harvested, embedded

doi: 10.1111/j.1349-7006.2010.01494.x

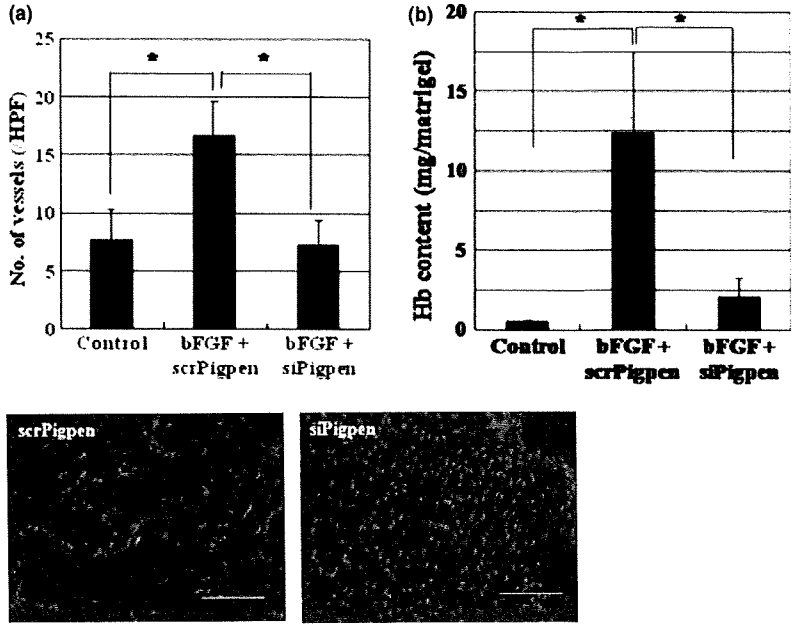

Fig. 6. Matrigel plug assay was performed as described in the Materials and Methods. On day 6, blood vessels positive for vascular endothelial (VE)-cadherin were counted (a) and hemoglobin content in the Matrigels was measured (b). Data indicate means and SEs (a) or SDs (b). $n = 12$ (Control) or 15 (basic fibroblast growth factor [bFGF] + scr- or siPigpen) in (a); $n = 5$ (Control and bFGF + siPigpen) or 6 (bFGF + siPigpen) in (b). $^*P < 0.05$. Representative immunohistochemistry (IHC) of VE-cadherin (red) and nuclei (blue) is shown. Scale bar = 100 μm. Hb, hemoglobin.

in OCT compound (Sakura Finetechnical, Tokyo, Japan), and snap-frozen in liquid nitrogen. Thin sections (5–6 μm) were cut on a cryostat (Leica CM1850, Leica MZFLIII; Leica Microsystems, Wetzlar, Germany) and collected on glass slides. Specimens were dried for 30 min and fixed in 4% PFA in 0.1 M PBS for 10 min. After washing with PBS, specimens were incubated in BS for 1 h, and then incubated with 2 μg/mL anti-VE-cadherin (Alexis Biochemicals, San Diego, CA, USA) or 1/100 (v/v) antimouse CD31 monoclonal (Fitzgerald Industries International, Concord, MA, USA) and 10 μg/mL antimouse pigpen rat IgG in RB for 1 h. After three washes with PBS, specimens were incubated with 4 μg/mL Alexa Fluor 546 goat antirabbit and rat IgG (Invitrogen) for VE-cadherin and CD31, respectively, or Alexa Fluor 488 goat antirabbit IgG (Invitrogen) for pigpen in RB for 1 h, washed with PBS three times, and incubated with Hoechst 33342 or TO-PRO-3 for nuclear staining. After a tap water rinse, VE-cadherin, CD31, and pigpen signals in endothelial cells were observed under a fluorescent microscope (Biozero BZ-8000, Keyence).

Statistical analysis. The statistical significance of differences was evaluated by ANOVA, and P-values were calculated using the Student's t-test. A value of $P < 0.05$ was considered statistically significant. The statistical calculation was done using JMP software (SAS, Cary, NC, USA).

Results

PILSAP activity regulated the expression of pigpen, a coiled body component protein. We previously showed that among vascular endothelial growth factor receptor 2 (VEGFR2)-positive precursor cells, including vascular, hematopoietic, and muscle lineages, only ECs continued to express VEGFR2 until terminal differentiation in an *in vitro* mouse ES differentiation culture system.[9] The time course of VEGFR2 expression in EBs showed two peaks at days 4 and 10, indicating expansion of VEGFR2-positive mesodermal precursors and endothelial lineages, respectively.[9] To clarify the mechanisms of how PILSAP plays a role in differentiation or maturation of ECs, we searched for molecules whose expression was correlated with the AP activity of PILSAP. On day 8, after day 7 when the expression of PILSAP was lowest and before day 10, the second peak when other EC markers including CD31 and Tie-2 peaked as well,[9] nuclear protein was extracted from mtPILSAP and mock EBs, and proteome analysis was performed. Pigpen was identified as a molecule whose expression was reduced to less than half in mtPILSAP EBs compared with mock EBs.

Binding of pigpen to PILSAP. The previous result that the AP activity of PILSAP regulates pigpen expression during EC differentiation does not necessarily indicate that pigpen directly interacts with PILSAP in ECs. Therefore, we examined whether pigpen could bind to PILSAP. Immunoprecipitation with anti-PILSAP followed by western blotting of pigpen and PILSAP demonstrated binding between these two molecules in a mouse endothelial cell line, MSS31. Furthermore, the binding was induced by a 20-min treatment with the representative angiogenic growth factors, VEGF and bFGF in ECs (Fig. 1a,b). Immunocytochemical analysis revealed that pigpen was localized in nuclei, whereas PILSAP was in cytosol and on nuclear membrane. VEGF and bFGF induced translocation of PILSAP from cytosol to nuclei (Fig. 1c). These results suggest that pigpen may be involved in angiogenesis in cooperation with PILSAP upon VEGF and bFGF stimuli.

SiRNA for pigpen inhibited *in vitro* angiogenesis. We next investigated whether pigpen plays a role in angiogenesis. We synthesized siRNAs for pigpen and their controls (siPigpen and scrPigpen; NC siRNA, siPigpen-A, and siPigpen-B). SiPigpen strongly inhibited the expression of pigpen protein in mouse endothelial cell lines, MSS31 and MS1 (Fig. 2a) as well as pigpen mRNA (data not shown). The protein level of PILSAP was not altered by transfection of siRNAs for pigpen. Transfection of siPigpen into MSS31 or MS1 abrogated the increase in proliferation by VEGF or bFGF, respectively (Fig. 3a). The decrease in EC proliferation by inhibiting pigpen expression was confirmed by two other siRNAs, namely siPigpen-A and siPigpen-B (Fig. 3b). Moreover, siPigpen significantly inhibited MS1 migration and abrogated the increase by VEGF (Fig. 4a). Inhibition of EC migration by the transfection with three different siRNAs was observed in MSS31 (Fig. 4b). Furthermore, siPigpen significantly inhibited network formation on Matrigel (Fig. 5). These data demonstrate the positive effect of pigpen on EC proliferation, migration, and network formation.

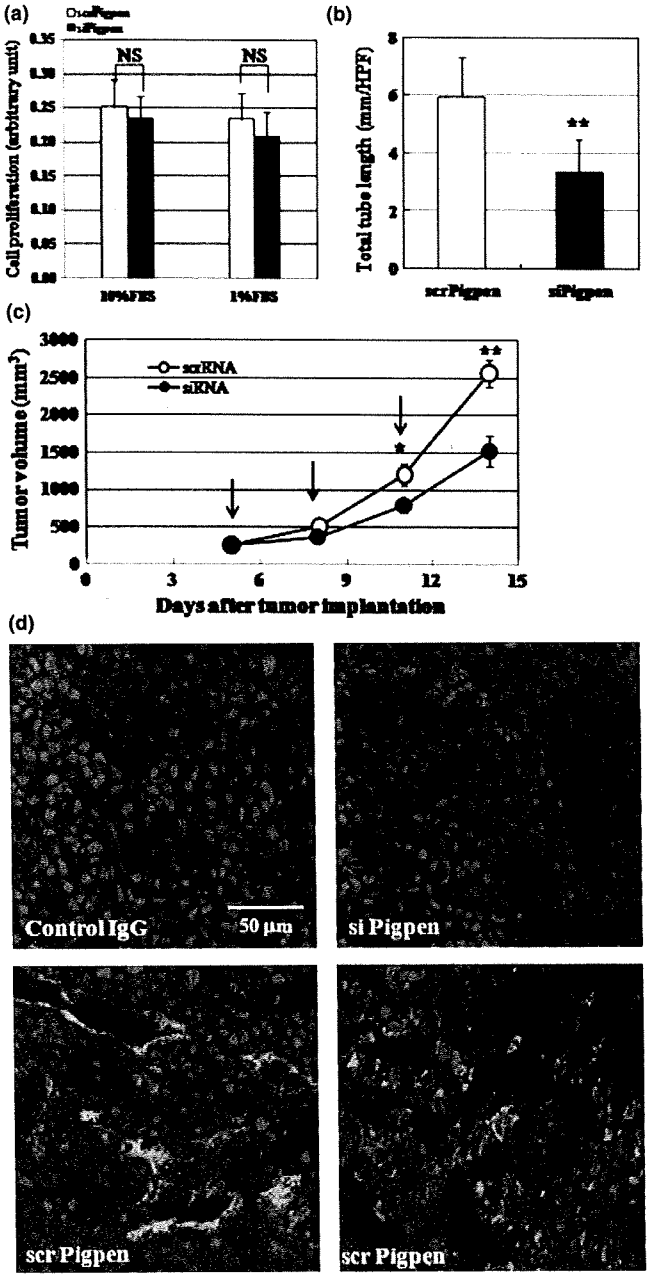

Fig. 7. Syngenic tumor implantation model was performed as described in the Materials and Methods. (a) siPigpen did not inhibit Lewis lung carcinoma (LLC) cell proliferation *in vitro*. Data indicate means and SDs, $n = 10$. (b) siPigpen inhibited tumor growth of LLC. Data indicate means and SEMs, $n = 10$ and 11 for scr- and siPigpen, respectively (days 5, 8, 10) and $n = 8$ (day 14). (c) siPigpen inhibited tumor angiogenesis. Data indicate means and SDs, $n = 15$ (scrPigpen) or 10 (siPigpen). $^*P < 0.05$, $^{**}P < 0.01$. (d) Representative immunohistochemistry (IHC) of CD31 (red), pigpen (green), and nuclei (blue) is shown. Bar = 50 μm.

SiRNA for pigpen inhibited *in vivo* angiogenesis. Next, we performed a Matrigel plug assay to examine the effect of siPigpen on *in vivo* angiogenesis. GFR-Matrigel containing 100 ng/mL bFGF, heparin, and 200 nM scr- or siPigpen was subcutaneously injected into 5-week-old mice. On day 6, Matrigel was removed, and we measured the Hb content and counted the number of blood vessels that were positive for VE-cadherin in transplanted GFR-Matrigel to analyze blood vessel formation and blood supply. Both the Hb content and blood vessel number were significantly increased by bFGF, and siPigpen abrogated this increase by bFGF (Fig. 6). Thus, pigpen appears to be involved in both *in vitro* and *in vivo* angiogenesis.

SiRNA for pigpen inhibited tumor growth as well as tumor angiogenesis. The result showing an inhibitory effect of siPigpen on *in vivo* angiogenesis prompted us to examine whether siPigpen could reduce tumor growth by inhibiting tumor angiogenesis. We employed a syngenic tumor implantation model of LLC. LLC cells express less pigpen than mouse ECs *in vitro* (Fig. 2a, scrPigpen) as well as *in vivo* (Fig. 7d, scrPigpen). Transfection of siPigpen into LLC cells did not alter the proliferation (Fig. 7a). LLC cells in GFR-Matrigel were subcutaneously injected into C57BL/6 mice. On day 5 when tumors became palpable, scr- or siPigpen was injected into the tumor, and the injection was repeated every three days. Figure 7(b) shows the time course of tumor growth in both groups. Injection of siPigpen significantly reduced the tumor size compared with the scrPigpen group on days 10 and 14, after two and three injections, respectively. Immunohistochemical analysis of tumor on day 14 showed the efficient inhibition of pigpen expression by siPigpen (Fig. 7d). The total tube length of blood vessels that were positive for CD31 on day 14 was significantly reduced by siPigpen injection (Fig. 7c,d). These data indicate that pigpen may be a future target for blocking tumor angiogenesis.

Discussion

We previously isolated PILSAP as a novel angiogenesis factor and showed that the expression of PILSAP is enhanced in mouse cells differentiating from ES cells to ECs.[5] We also demonstrated that PILSAP is involved in postnatal angiogenesis.[5–8] In this study, we searched for a molecule that is related to PILSAP and involved in endothelial differentiation, similar to PILSAP. Proteome analysis using mtPILSAP and mock EBs on day 8 of *in vitro* differentiation cultures revealed that the expression of pigpen, a nuclear coiled body component, was reduced to less than half in mtPILSAP EBs lacking the AP activity. This result suggests that AP activity of PILSAP may regulate pigpen expression, but does not indicate that pigpen directly interacts with PILSAP. However, we detected the complex of PILSAP and pigpen in the nuclear and membrane fractions of EBs and found that the binding was down-regulated in mtPILSAP-EBs (M. Abe, unpublished data, 2008). Pigpen has been suggested to be involved in angiogenesis, especially by inducing EC proliferation and differentiation.[10,11,14,15,16] Therefore, we speculated that pigpen might play a role in angiogenesis in cooperation with PILSAP. First, we examined whether pigpen could bind to PILSAP using IP-Western blotting of mouse EC protein extracts. Although it is known that PILSAP is a cytosolic enzyme[5] and pigpen is a nuclear protein,[11] western blotting using fractionated cell lysates of mouse EBs and ECs revealed that PILSAP localizes predominantly in the cytosol and membrane fractions, whereas pigpen localizes in the nuclear and membrane fractions (M. Abe, unpublished data, 2008). Moreover, ICC of PILSAP and pigpen in MSS31 showed their localization, namely cytosol/nuclear membrane and nucleus/nuclear membrane, respectively (Fig. 1c). The binding of these two molecules were augmented by VEGF and bFGF (Fig. 1a,b). ICC of these molecules demonstrated that VEGF and bFGF induced PILSAP translocation from cytosol to the nucleus/nuclear membrane where pigpen

doi: 10.1111/j.1349-7006.2010.01494.x

existed (Fig. 1c), although bFGF showed less effect compared with VEGF in these experiments with 20-min incubation (Fig. 1).

Next, we investigated whether pigpen plays a role in postnatal angiogenesis as PILSAP. Three different siRNAs for pigpen inhibited proliferation and migration of MSS31 (Figs 3b and 4b). Although PILSAP regulated pigpen expression, pigpen did not alter PILSAP expression (Fig. 2b). Transfection of siPigpen, one of these siRNAs, inhibited proliferation and migration of two different cell types, MSS31 and MS1, and abrogated the increase in proliferation and migration by VEGF and bFGF (Figs 3–4). Inhibition of pigpen expression resulted in suppression of angiogenesis both *in vitro* (Figs 3–5) and *in vivo* (Fig. 6). Furthermore, injection of siPigpen in syngenic tumors subcutaneously implanted into C57BL/6 mice inhibited tumor growth and tumor angiogenesis (Fig. 7). These findings suggest that the inhibition of pigpen may be useful for therapy of malignant tumors by inhibiting tumor angiogenesis.

We speculate that PILSAP–pigpen complex induced by VEGF and bFGF may play a role in angiogenesis. Further study is needed to clarify whether and how pigpen interacts with PILSAP to promote angiogenesis *in vivo* and whether pigpen is a substrate for PILSAP.

Acknowledgments

This work was supported in part by a Grant-in-Aid for Scientific Research (no. 17590235) from the Ministry of Education, Science, Sports and Culture of Japan.

Disclosure Statement

The authors have no conflict of interest.

References

1 Folkman J. Tumor angiogenesis: therapeutic implications. *N Engl J Med* 1971; **285**: 1182–6.
2 Bergers G, Benjamin LE. Tumorigenesis and the angiogenic switch. *Nat Rev Cancer* 2003; **3**: 401–10.
3 Carmeliet P, Ferreira V, Breier G *et al.* Abnormal blood vessel development and lethality in embryos lacking a single VEGF allele. *Nature* 1996; **380**: 435–9.
4 Ferrara N, Carver-Moore K, Chen H *et al.* Heterozygous embryonic lethality induced by targeted inactivation of the VEGF gene. *Nature* 1996; **380**: 439–42.
5 Miyashita H, Yamazaki T, Akada T *et al.* A mouse orthologue of puromycin-insensitive leucyl-specific aminopeptidase is expressed in endothelial cells and plays an important role in angiogenesis. *Blood* 2002; **99**: 3241–9.
6 Yamazaki T, Akada T, Niizeki O, Suzuki T, Miyashita H, Sato Y. Puromycin-insensitive leucyl-specific aminopeptidase (PILSAP) binds and catalyzes PDK1, allowing VEGF-stimulated activation of S6K for endothelial cell proliferation and angiogenesis. *Blood* 2004; **104**: 2345–52.
7 Akada T, Yamazaki T, Miyashita H *et al.* Puromycin insensitive leucyl-specific aminopeptidase (PILSAP) is involved in the activation of endothelial integrins. *J Cell Physiol* 2002; **193**: 253–62.
8 Suzuki T, Abe M, Miyashita H, Kobayashi T, Sato Y. Puromycin insensitive leucyl-specific aminopeptidase (PILSAP) affects RhoA activation in endothelial cells. *J Cell Physiol* 2007; **211**: 708–15.
9 Abe M, Sato Y. Puromycin insensitive leucyl-specific aminopeptidase (PILSAP) is required for the development of vascular as well as hematopoietic system in embryoid bodies. *Genes Cells* 2006; **11**: 719–29.
10 Alliegro MC, Alliegro MA. A nuclear protein regulated during the transition from active to quiescent phenotype in cultured endothelial cells. *Dev Biol* 1996; **174**: 288–97.
11 Alliegro MC, Alliegro MA. Identification of a new coiled body component. *Exp Cell Res* 1996; **227**: 386–90.
12 Alliegro MC, Alliegro MA. Protein heterogeneity in the coiled body compartment. *Exp Cell Res* 1998; **239**: 60–8.
13 Ogg SC, Lamond AI. Cajal bodies and coilin–moving towards function. *J Cell Biol* 2002; **159**: 17–21.
14 Blank M, Weinschenk T, Priemer M, Schluesener H. Systematic evolution of a DNA aptamer binding to rat brain tumor microvessels. selective targeting of endothelial regulatory protein pigpen. *J Biol Chem* 2001; **276**: 16464–8.
15 Alliegro MC, Alliegro MA. Nuclear injection of anti-pigpen antibodies inhibits endothelial cell division. *J Biol Chem* 2002; **277**: 19037–41.
16 Alliegro MC. Pigpen and endothelial cell differentiation. *Cell Biol Int* 2001; **25**: 577–84.

Biochemical and Biophysical Research Communications 380 (2009) 609–613

Contents lists available at ScienceDirect

Biochemical and Biophysical Research Communications

journal homepage: www.elsevier.com/locate/ybbrc

Identification and characterization of stem cell-specific transcription of *PSF1* in spermatogenesis

Yinglu Han, Masaya Ueno, Yumi Nagahama, Nobuyuki Takakura *

Department of Signal Transduction, Research Institute for Microbial Diseases, Osaka University, 3-1, Yamada-oka, Suita, Japan

ARTICLE INFO

Article history:
Received 22 January 2009
Available online 27 January 2009

Keywords:
DNA replication
Testis development
Promoter
PSF1
Stem cell

ABSTRACT

PSF1 is an evolutionarily conserved DNA replication factor, which forms the GINS complex with PSF2, PSF3, and SLD5. The mouse *PSF1* homolog has been identified from a stem cell-specific cDNA library. To investigate its transcriptional regulatory mechanisms during differentiation, we studied *PSF1* mRNA expression in testis and characterized its promoter. No canonical TATA or CAAT boxes could be found in the *PSF1* 5′-flanking region, whereas several consensus AML1, GATA, and Sry putative binding sequences are predicted within 5 kb of the putative transcription start site. In addition, binding sites for oncoproteins such as Myb and Ets were also found in the promoter. In testis, various *PSF1* gene transcription initiation sites are present and short transcripts encoding two novel isoforms, PSF1b and 1c, were found. However, spermatogonium stem cells specifically express transcripts for PSF1a. These data suggest that PSF1 is tightly regulated at the transcriptional level in stem cells.

Because of the finite life span of most mature cells, tissue stem cells, and progenitors are required to supply replacements by proliferation and differentiation. Particularly, testis and bone marrow (BM) stem cells continuously self-renew and also produce differentiated cell lineages. Hematopoietic stem cells (HSCs) and spermatogonial stem cells (SSCs) have a high regenerative capacity. In a mouse experimental model, one single HSC was found to be sufficient to reconstitute hematopoiesis when transplanted into a BM-ablated recipient [1]. When spermatogenesis is disrupted by high temperatures or drugs, surviving SSCs can regenerate spermatogenesis [2,3]. Because these tissue stem cells have great regenerative capacity for reconstituting ablated tissues, ex vivo amplification of stem cells without loss of self-renewal and multidifferentiation potential represents an important target for transplantation, gene, and cellular therapies. In order to study the molecular mechanisms regulating self-renewal of stem cells, knock-out (KO) mice lacking several cell cycle-related genes, such as p27, p18, and ATM, were generated as previously reported [4–6]. However, their downstream function in the self-renewal process, especially regarding molecules involved in DNA replication, is currently not known.

The initiation of DNA replication in eukaryotic cells is mediated by a highly ordered series of steps involving multiple complexes at replication origins [7,8]. This process commences with the binding of the origin recognition complex (ORC) to replication origins. CDC6 and Cdt1 bind to ORCs to act as loading factors for the Mcm2-7 (minichromosome maintenance) complex and then pre-replication complexes (pre-RC) are established. At the G1/S transition of the cell cycle, the pre-RCs are transformed into initiation complexes (ICs). Activation of MCM helicase activity requires the action of two protein kinases, DDK (Cdc7-Dbf4) and CDK (cyclin-dependent), as well as the participation of at least eight additional factors, including Mcm10, Cdc45, Dpb11, synthetic lethal with dpb11 mutant-2 (Sld2), Sld3, and GINS [9]. GINS was recently identified as a novel heterotetrameric complex from lower eukaryotes. It consists of four subunits, SLD5, PSF1, PSF2, and PSF3, each of approximately 200 amino acid residues highly conserved in all eukaryotes and essential for both the initiation and progression of DNA replication [10–12].

By using lower eukaryote models, multiple steps for progression of DNA replication are now well understood at the protein level, e.g. phosphorylation, degradation, and/or interaction processes; however, how these factors are activated or inactivated at the RNA level in mammalian tissues consisting of multiple cell lineages and cells in different phases of the cycle has not been elucidated. Previously, we cloned the mouse ortholog of *PSF1* and *SLD5* from an HSC-specific cDNA library or by two-hybrid screening of a cDNA library derived from embryos [13,14]. Transcription of *PSF1* is predominantly found in highly proliferative tissues, such as BM and testis. Loss of *PSF1* causes embryonic lethality around the implantation stage [13], with *PSF1*$^{-/-}$ embryos showing impaired proliferation of multipotent stem cells, i.e., the inner cell mass. However, the transcriptional regulation of *PSF1* in immature cells is not understood.

Abbreviations: GINS, Go-ichi-nii-san; PSF, partner of SLD5; SSCs, sperm stem cells; HSCs, hematopoietic stem cells

* Corresponding author. Fax: +81 6 6879 8314.
E-mail address: ntakaku@biken.osaka-u.ac.jp (N. Takakura).

0006-291X/$ - see front matter © 2009 Elsevier Inc. All rights reserved.
doi:10.1016/j.bbrc.2009.01.133

Here, we have isolated the 5′ promoter sequence of the *PSF1* gene to investigate regulatory mechanisms responsible for tissue-specific expression. We report an in silico analysis of the potential *cis*-regulatory elements in the *PSF1* promoter. In addition, we studied SSC-specific transcription initiation sites and multiple transcription initiation sites of *PSF1* in testis.

Materials and methods

Animals. ICR mice were purchased from Japan SLC (Shizuoka, Japan). All animal studies were approved by the Osaka University Animal Care and Use Committee.

In situ hybridization. cDNA fragments were amplified by PCR using the primer set 5′-GAA TTC AAA GCT TTG TAT GAA CAA AAC CAG-3′ and 5′-GTC GAC TCA GGA CAG CAC GTG CTC TAG AAC T-3′, followed by ligation into pT7 Blue Vector (Novagen Inc., Madison, WI, USA). These plasmids were used for probe synthesis. Antisense and sense cRNA probes were synthesized using digoxigenin (DIG)-RNA labeling kits with T7 RNA polymerase (Roche Diagnostics, Indianapolis, IN, USA). Hybridization was performed as previously described [15].

Cell culture. Colon 26 cells were maintained in DMEM medium containing 10% FBS, 100 IU penicillin and 100 μg/ml streptomycin. The cells were plated in 10 cm tissue culture dishes in 5% CO_2 and 95% air at 37 °C.

5′-Rapid amplification of cDNA ends (5′-RACE). 5′-RACE was performed as described previously [16]. In brief, we used the 5′ RACE System for Rapid Amplification of cDNA Ends (Invitrogen, Carlsbad, CA) according to the manufacturer's instructions. Total RNA was purified from whole testis, embryonic day (E) 10.5 embryos, colon 26 cells, and sorted cells (see below) by the guanidine-thiocyanate extraction method. Total RNA of sorted cells was purified using RNeasy Plus Mini Kits (Qiagen, Valencia, CA) according to manufacturer's instructions. *PSF1* transcripts were reverse-transcribed with Superscript II (Invitrogen) using the gene-specific primer PSF1GSP1 5′-GCA TGT CTG TCA ATT TAA-3′. The products were poly(C) tailed by terminal deoxynucleotidyl transferase and amplified by PCR, using an anchor primer and the gene-specific primer 5′-CGA AGC AAC CGG TCA TAC A-3′ (PSF1ANGSP1). The amplified products were subcloned into pT7 Blue vector (Novagen).

5′ End amplification of PSF1 cDNA using 5′ End oligo-capped cDNA library. CapSite cDNA (Nippon Gene., Toyama, Japan) from mouse testis and embryo (Day15) was used as a template for PCR with primer 1RC (Nippon gene., Toyama, Japan) corresponding to the oligoribonucleotide sequence ligated at the cap site and a *PSF1* gene-specific primer, 5′-CGA AGC AAC CGG TCA TAC A-3′ (PSF1ANGSP1) and the PCR product was then used as a template for the second round PCR with nested primers 2RC (Nippon Gene) and 5′-GCTATCGTGCAGCGTCTATT-3′ (PSF1ANGSP2). The amplified products were used for Southern blotting or purified, cloned and sequenced.

Southern blotting. Amplified 5′-ends of cDNA by 5′-RACE (see above) were separated on 0.8% agarose gels and transferred onto nylon membrane filters which were hybridized overnight at 60 °C in DIG Easy Hyb (Roche Diagnostics, Germany) with a digoxigenin-labeled *PSF1* cDNA probe. The hybridized probe was detected with alkaline phosphatase-conjugated antidigoxigenin antibodies using the DIG luminescent detection kit (Roche), following the manufacturer's instructions. The probe was prepared by using PCR DIG Probe Synthesis Kits (Roche) with primers: E11prb-2s (5′-AGC TGG TTG CTG GTG TTG TGC GAC-3′) and E11prb-2r (5′-CGA AAA CAA GAA ACG CTC AGA TGG G-3′).

Enrichment of SSCs. Isolation of SSCs was as previously reported [17]. Briefly, experimental cryptorchid testes were produced by suturing the testis fat pad to the abdominal wall at 7 weeks of age. After 2 or 3 months, testes were dissected and then digested with collagenase (Type IV, Sigma, St Louis, MO) at 32 °C for 15 min. The cells were next digested with DNase (Sigma) and trypsin (GIBCO) at 32 °C for 10 min. When most of the cells were dispersed, the action of trypsin was terminated by adding PBS containing 1% fetal bovine serum. Cell sorting was performed as described previously [18]. The antibody used for detection of SSCs was a FITC-conjugated anti-α6-integrin antibody (BD Biosciences. San Jose, CA). Control cells were stained with isotype-matched control antibodies. After the final wash, cells were resuspended in 2 ml of PBS/FBS containing 1 μg/ml propidium iodide for identification of dead cells. The stained cells were analyzed by FACS Calibur (Becton & Dickinson, New Jersey, USA), and sorted by JSAN (Bay Bioscience, Kobe, Japan).

Results and discussion

Proliferating germ cells express high levels of PSF1 transcripts

Previously we reported that *PSF1* transcripts are highly expressed in testis and BM [13]. In addition, immunohistochemistry also revealed the presence of PSF1 protein specifically in the spermatogonia, lining the outermost layer of the testis [13]. Here, to study the expression of *PSF1* mRNA in the testis, we performed in situ hybridization with an antisense-probe which hybridized to spermatogonia (arrow) and spermatocytes (arrowhead) (Fig. 1A). No obvious signals were recorded when using the sense-probe (Fig. 1B). These data indicate that stem cell-specific expression of PSF1 may be regulated at the transcriptional or post-transcriptional level, because although PSF1 protein could be detected in the spermatogonia this was not the case in spermatocytes [13].

Identification and characterization of PSF1 transcription initiation sites

In order to identify the *PSF1* promoter, we performed 5′-RACE analysis with *PSF1* gene-specific primers. Total RNA from testis, colon 26 cells, and whole embryo were reverse-transcribed (see Materials and methods). Although a single DNA band <372 bp in length was obtained after nested PCR of colon 26 and whole embryo, a broad band was amplified from testis cDNA (Fig. 1C,a). We also observed smaller transcripts in 5′ End amplificated cDNA of *PSF1* using 5′ End oligo-capped cDNA library from testis compared to that from embryo (Fig. 1C,b). To exclude that this was caused by degraded RNA in our sample, total RNA was visualized by Ethidum bromide (Fig. 1D). The quality of the RNA in each sample was essentially the same. Thus, the broad band seen in testis was not caused by RNA degradation. We then amplified each cDNA fragment, purified them and subcloned them for DNA sequencing. Here, the 5′-end of the longest cDNA fragment is defined as "+1" (Table 1, +1 5′-TGC ACT TCT ATT-3"). It was located 157 bp upstream of the first ATG.

Putative cis elements of the 5′-flanking regions of PSF1

To characterize the 5′-flanking region of PSF1, we analyzed putative transcription binding sites in silico (Fig. 3). The proximal 5′-flanking region of the *PSF1* gene lacks consensus CAAT or TATA boxes, but possesses consensus Sp1 binding sites, which are characteristic of TATA-less gene promoters [19]. In the 5′-flanking region of *PSF1*, several putative *cis*-acting elements were identified, such as E2F, GATA, Myb, AML1, Evi-1, and Sry.

As previously reported, E2F is known to regulate DNA replication, cell cycle progression, DNA repair, and differentiation

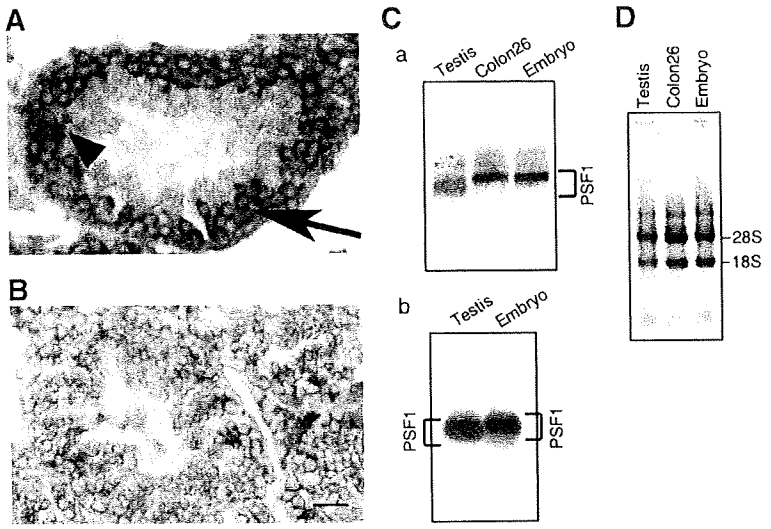

Fig. 1. *PSF1* expression in adult testis. (A) Antisense or (B) sense-probes for detection of *PSF1* were hybridized on sections of adult testis. Arrow, spermatogonia; arrowhead, spermatocyte. Bar indicates 20 μm. (C) Southern blot analysis of 5′-RACE product (a) and 5′ End amplificated cDNA of *PSF1* using 5′ End oligo-capped cDNA library (b) hybridized with a *PSF1* cDNA probe. Note that diffuse short bands are found in testis. (D) Ethidium bromide staining of total RNAs used in (C).

Table 1
Positions of 5′-RACE products of PSF1 transcripts.

Tissue or cells	Position of 5′-end	Translation		
		PSF1a	PSF1b	PSF1c
Colon 26	1, 20, 20, 20, 30, 30, 37, 42, 70, 70, 74, 227	92	0	8
Embryo	20, 30, 30, 30, 32, 35, 38, 47, 49, 50, 53, 57, 66, 72, 73, 117, 160	94	6	0
Testis	16, 22, 24, 25, 28, 28, 30, 30, 36, 66, 70, 70, 70, 70, 71, 73, 73, 73, 100, 107, 107, 113, 113, 113, 113, 113, 121, 130, 130, 146, 155, 155, 155, 161, 165, 165, 165, 165, 165, 165, 178, 178, 182, 182, 182, 182, 182, 186, 191, 193, 193, 193, 193, 213, 227, 230	59	13	28
SSCs	ND[a]	100[b]	0[b]	0[b]

[a] ND, No data.
[b] Percents are determined by PCR.

[20,21]. Moreover, E2F-1 is expressed in $CD34^+$ human hematopoietic stem and progenitor cells [22], and may play a critical role in hematopoiesis. Myb, AML1, and Evi-1 are also essential for HSC development [23–25]. GATA-1 does have a critical role in fate decision of HSCs [26]. Although GATA-2 has been suggested to play a role in maintenance of HSCs from the observation of GATA-$2^{-/-}$ mice [27], it remains indeterminate whether GATA-2 enhances or suppresses the growth of HSCs [28–31]. As high level expression of PSF1 is observed in hematopoietic organs and testis in the adulthood, suggesting that these transcription factors may contribute to stem cell-specific transcription in testis as well as hematopoietic organs.

Multiple translation initiation sites

In our 5′-RACE analysis, small cDNA fragments were found specifically in testis (Fig. 2 and Table 1). Therefore, we next analyzed the translation initiation sites of each cDNA fragment (Fig. 3 and Table 1). ATG was present first in most of the transcripts tested in colon 26 and whole embryo, suggesting that these are translated to full-length PSF1 (PSF1a). However, in testis, there were many short transcripts which may be translated to truncated forms of PSF1 (PSF1b or PSF1c). Putative PSF1b lacks 6 amino acid residues and putative PSF1c lacks a partial portion of a coiled-coil domain compared to the PSF1 protein. The DNA sequences from the RT-PCR products of 5′ End amplifications using 5′ End oligo-capped cDNA library showed that 1.2% of the transcripts derived from testis were PSF1a type and the remnants were PSF1b and PSF1c. On the other hand, transcripts derived from embryo were almost exclusively PSF1a type. These data suggest that the short PSF1 transcripts may be translated into the truncated forms PSF1b and PSF1c specifically in testis.

SSCs express only the PSF1a isotype

Next, to investigate which RNAs are transcribed in sperm stem cells (SSCs, spermatogonia), we sorted these cells (Fig. 4A) and performed 5′-RACE analysis (Fig. 4B and Table 1). In contrast to whole testis, only one band was amplified from SSCs. After purification, we assessed the cDNA using PCR and found that amplificates contained ATG first, suggesting that only PSF1a is expressed in SSCs (Table 1).

We detected PSF1 protein in spermatogonia but not in spermatocytes by immunohistochemical analysis [13], although in situ hybridization revealed that primary and secondary spermatocytes as well as spermatogonia contained PSF1 transcripts. We found that SSCs express PSF1a but not PSF1b or PSF1c. These results suggest that the PSF1b and 1c RNA which is present in primary and secondary spermatocytes may be unstable and degrade easily.

In summary, we identified several *PSF1* transcription initiation sites. Various small cDNA fragments of *PSF1* were derived from testis, suggesting that *PSF1* RNAs are translated into three isotypes. These alternative forms may generate functionally different PSF1 proteins, contributing to differences in the mechanism of prolifer-

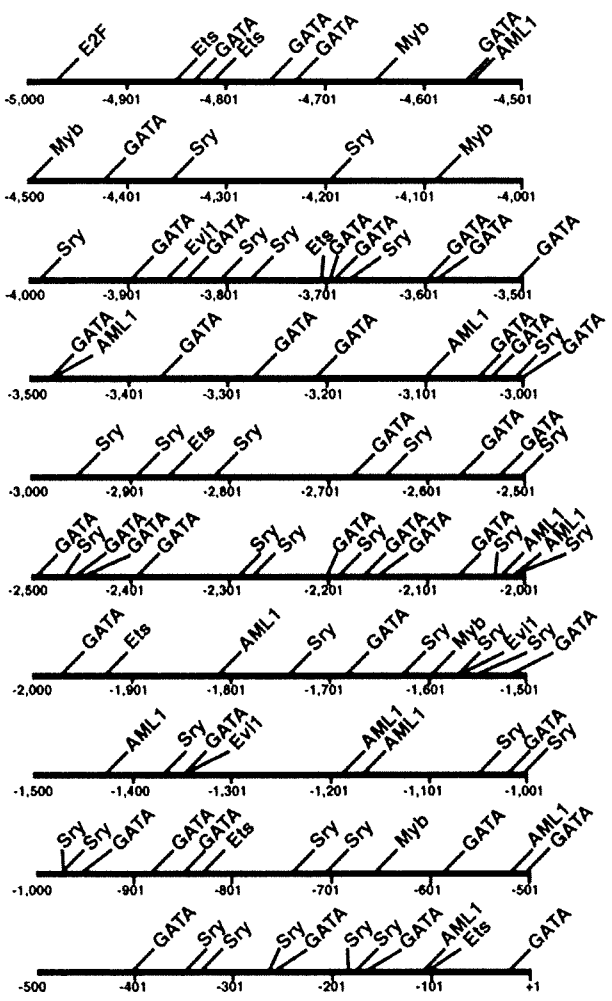

Fig. 2. Schematic representation of the putative transcriptional regulatory elements in the 5′-flanking region of the mouse *PSF1* gene. Consensus sequences of *cis*-regulatory elements in the *PSF1* promoter were sought in the TFSEARCH database (http://mbs.cbrc.jp/research/db/TFSEARCH.html). The numbers in parentheses indicate the positions of the first and last nucleotides of the elements.

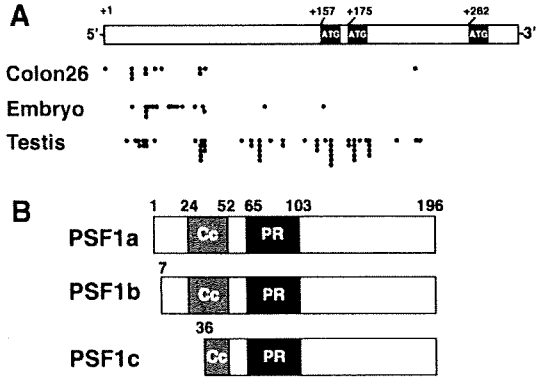

Fig. 3. Transcription initiation sites of *PSF1* and PSF1 isoforms. (A) Schematic representation of the summed data on transcription initiation sites. Each closed dot indicates the position of 5′-ends of 5′-RACE products. (B) Putative primary structures of PSF1 isoforms. Cc, N terminal region containing coiled-coil domain; PR, central region containing arginine-rich domain.

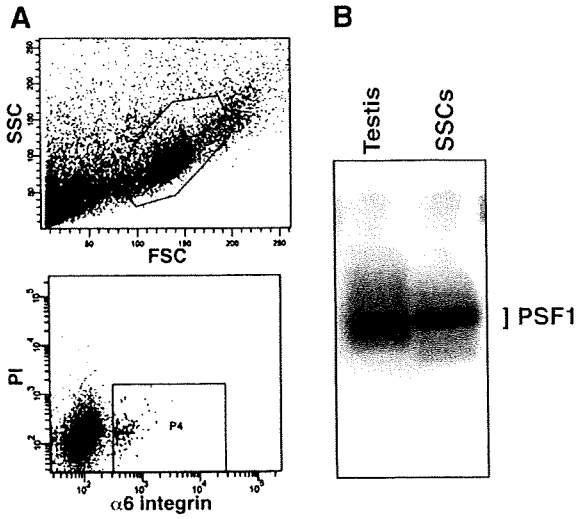

Fig. 4. Expression of *PSF1* gene in SSCs. (A) Flow cytometric analysis for sorting SSCs. Gated region for SSCs in SSC/FSC (upper) and α6-integrin$^+$ PI$^-$ cells population (lower) is shown. (B) Southern blot analysis of 5′-RACE products hybridized with a *PSF1* cDNA probe. Diffuse short bands were found in whole testis (Testis). SSCs, spermatogonium stem cells.

ation control in stem cells and progenitor cells. Further analysis of the regulatory mechanisms influencing PSF1 expression are needed to shed more light on the complex mechanisms of "stemness" in mammalian cells.

Acknowledgments

We thank N. Fujimoto, Y. Shimizu, K. Ishida, M. Sato, and Y. Nakano for technical assistance. We also thank K. Fukuhara for secretarial assistance. This work was partly supported by the Japanese Ministry of Education, Culture, Sports, Science and Technology, and the Japan Society for Promotion of Science.

References

[1] M. Osawa, K. Hanada, H. Hamada, H. Nakauchi, Long-term lymphohematopoietic reconstitution by a single CD34-low/negative hematopoietic stem cell, Science 273 (1996) 242–245.
[2] Y. Nishimune, S. Aizawa, T. Komatsu, Testicular germ cell differentiation in vivo, Fertil. Steril. 29 (1978) 95–102.
[3] C.J. van Keulen, D.G. de Rooij, Spermatogonial stem cell renewal in the mouse. II. After cell loss, Cell Tissue Kinet. 6 (1973) 337–345.
[4] T. Cheng, Rodrigues N.S. Stier, D.T.. Scadden, Stem cell repopulation efficiency but not pool size is governed by p27 (kip1), Nat. Med. 6 (2000) 1235–1240.
[5] Y. Yuan, H. Shen, D.S. Franklin, D.T. Scadden, T. Cheng, In vivo self-renewing divisions of haematopoietic stem cells are increased in the absence of the early G1-phase inhibitor, p18INK4C, Nat. Cell Biol. 6 (2004) 436–442.
[6] K. Ito, A. Hirao, F. Arai, S. Matsuoka, K. Takubo, I. Hamaguchi, K. Nomiyama, K. Hosokawa, K. Sakurada, N. Nakagata, Y. Ikeda, T.W. Mak, T. Suda, Regulation of oxidative stress by ATM is required for self-renewal of haematopoietic stem cells, Nature 431 (2004) 997–1002.
[7] J.J. Blow, A. Dutta, Preventing re-replication of chromosomal DNA, Nat. Rev. Mol. Cell Biol. 6 (2005) 476–486.
[8] T.S. Takahashi, D.B. Wigley, J.C. Walter, Pumps, paradoxes and ploughshares: mechanism of the MCM2–7 DNA helicase, Trends Biochem. Sci. 30 (2005) 437–444.
[9] K. Labib, A. Gambus, A key role for the GINS complex at DNA replication forks, Trends Cell Biol. 17 (2007) 271–278.
[10] M. Kanemaki, A. Sanchez-Diaz, A. Gambus, K. Labib, Functional proteomic identification of DNA replication proteins by induced proteolysis in vivo, Nature 423 (2003) 720–724.
[11] Y. Kubota, Y. Takase, Y. Komori, Y. Hashimoto, T. Arata, Y. Kamimura, H. Araki, H. Takisawa, A novel ring-like complex of Xenopus proteins essential for the initiation of DNA replication, Genes Dev. 17 (2003) 1141–1152.
[12] Y. Takayama, Y. Kamimura, M. Okawa, S. Muramatsu, A. Sugino, H. Araki, H. Takisawa, GINS, a novel multiprotein complex required for chromosomal DNA replication in budding yeast, Genes Dev. 17 (2003) 1153–1165.

[13] M. Ueno, M. Itoh, L. Kong, K. Sugihara, M. Asano, N. Takakura, PSF1 is essential for early embryogenesis in mice, Mol. Cell. Biol. 25 (2005) 10528–10532.
[14] L. Kong, M. Ueno, M. Itoh, K. Yoshioka, N. Takakura, Identification and characterization of mouse PSF1-binding protein, SLD5, Biochem. Biophys. Res. Commun. 339 (2006) 1204–1207.
[15] N. Kimura, M. Ueno, K. Nakashima, T. Taga, A brain region-specific gene product Lhx6.1 interacts with Ldb1 through tandem LIM-domains, J. Biochem. 126 (1999) 180–187.
[16] M. Ueno, N. Kimura, K. Nakashima, F. Saito-Ohara, J. Inazawa, T. Taga, Genomic organization, sequence and chromosomal localization of the mouse Tbr2 gene and a comparative study with Tbr1, Gene 254 (2000) 29–35.
[17] T. Shinohara, K.E. Orwig, M.R. Avarbock, R.L. Brinster, Spermatogonial stem cell enrichment by multiparameter selection of mouse testis cells, Proc. Natl. Acad. Sci. USA 97 (2000) 8346–8351.
[18] N. Takakura, T. Watanabe, S. Suenobu, Y. Yamada, T. Noda, Y. Ito, M. Satake, T. Suda, A role for hematopoietic stem cells in promoting angiogenesis, Cell 102 (2000) 199–209.
[19] S.T. Smale, Transcription initiation from TATA-less promoters within eukaryotic protein-coding genes, Biochim. Biophys. Acta 1351 (1997) 73–88.
[20] N. Dyson, The regulation of E2F by pRB-family proteins, Genes Dev. 12 (1998) 2245–2262.
[21] B.D. Rowland, R. Bernards, Re-evaluating cell-cycle regulation by E2Fs, Cell 127 (2006) 871–874.
[22] U. Steidl, R. Kronenwett, U.P. Rohr, R. Fenk, S. Kliszewski, C. Maercker, P. Neubert, M. Aivado, J. Koch, O. Modlich, H. Bojar, N. Gattermann, R. Haas, Gene expression profiling identifies significant differences between the molecular phenotypes of bone marrow-derived and circulating human CD34+ hematopoietic stem cells, Blood 99 (2002) 2037–2044.
[23] M.L. Mucenski, K. McLain, A.B. Kier, S.H. Swerdlow, C.M. Schreiner, T.A. Miller, D.W. Pietryga, W.J. Scott Jr., S.S. Potter, A functional c-myb gene is required for normal murine fetal hepatic hematopoiesis, Cell 65 (1991) 677–689.
[24] T. Okuda, J. van Deursen, S.W. Hiebert, G. Grosveld, J.R. Downing, AML1, the target of multiple chromosomal translocations in human leukemia, is essential for normal fetal liver hematopoiesis, Cell 84 (1996) 321–330.
[25] P.R. Hoyt, C. Bartholomew, A.J. Davis, K. Yutzey, L.W. Gamer, S.S. Potter, J.N. Ihle, M.L. Mucenski, The Evi1 proto-oncogene is required at midgestation for neural, heart, and paraxial mesenchyme development, Mech. Dev. 65 (1997) 55–70.
[26] H. Iwasaki, K. Akashi, Myeloid lineage commitment from the hematopoietic stem cell, Immunity 26 (2007) 726–740.
[27] F.Y. Tsai, G. Keller, F.C. Kuo, M. Weiss, J. Chen, M. Rosenblatt, F.W. Alt, S.H. Orkin, An early haematopoietic defect in mice lacking the transcription factor GATA-2, Nature 371 (1994) 221–226.
[28] C. Heyworth, K. Gale, M. Dexter, G. May, T. Enver, A GATA-2/estrogen receptor chimera functions as a ligand-dependent negative regulator of self-renewal, Genes Dev. 13 (1999) 1847–1860.
[29] S. Ezoe, I. Matsumura, S. Nakata, K. Gale, K. Ishihara, N. Minegishi, T. Machii, T. Kitamura, M. Yamamoto, T. Enver, Y. Kanakura, GATA-2/estrogen receptor chimera regulates cytokine-dependent growth of hematopoietic cells through accumulation of p21(WAF1) and p27(Kip1) proteins, Blood 100 (2002) 3512–3520.
[30] K. Kitajima, M. Masuhara, T. Era, T. Enver, T. Nakano, GATA-2 and GATA-2/ER display opposing activities in the development and differentiation of blood progenitors, EMBO J. 21 (2002) 3060–3069.
[31] D.A. Persons, J.A. Allay, E.R. Allay, R.A. Ashmun, D. Orlic, S.M. Jane, J.M. Cunningham, A.W. Nienhuis, Enforced expression of the GATA-2 transcription factor blocks normal hematopoiesis, Blood 93 (1999) 488–499.

Both alleles of *PSF1* are required for maintenance of pool size of immature hematopoietic cells and acute bone marrow regeneration

Masaya Ueno,[1] Machiko Itoh,[2] Kazushi Sugihara,[3] Masahide Asano,[3] and Nobuyuki Takakura[1,2]

[1]Department of Signal Transduction, Research Institute for Microbial Diseases, Osaka University, Osaka; [2]Department of Stem Cell Biology, Cancer Research Institute, Kanazawa University, Kanazawa; and [3]Institute for Experimental Animals, Kanazawa University Advanced Science Research Center, Kanazawa, Japan

Hematopoietic stem cells (HSCs) have a very low rate of cell division in the steady state; however, under conditions of hematopoietic stress, these cells can begin to proliferate at high rates, differentiate into mature hematopoietic cells, and rapidly reconstitute ablated bone marrow (BM). Previously, we isolated a novel evolutionarily conserved DNA replication factor, *PSF1* (*partner of SLD5-1*), from an HSC-specific cDNA library. In the steady state, PSF1 is expressed predominantly in CD34$^+$KSL (c-kit$^+$/Sca-1$^+$/Lineage$^-$) cells and progenitors, whereas high levels of PSF1 expression are induced in KSL cells after BM ablation. In 1-year-old *PSF1*$^{+/-}$ mice, the pool size of stem cells and progenitors is decreased. Whereas young *PSF1*$^{+/-}$ mutant mice develop normally, are fertile, and have no obvious differences in hematopoiesis in the steady state compared with wild-type mice, intravenous injection of 5-fluorouracil (5-FU) is lethal in *PSF1*$^{+/-}$ mice, resulting from a delay in induction of HSC proliferation during ablated BM reconstitution. Overexpression studies revealed that PSF1 regulates molecular stability of other GINS components, including SLD5, PSF2, and PSF3. Our data indicate that PSF1 is required for acute proliferation of HSCs in the BM of mice. (Blood. 2009;113:555-562)

Introduction

Tissue regeneration is one of the most tightly controlled processes requiring an ordered program involving induction of proliferation and differentiation of damaged-tissue stem cells. In the normal state, hematopoietic stem cells (HSCs) undergo cell division at a very low rate. However, if the bone marrow (BM) is ablated by an anticancer drug or radioactivity, HSCs that are in a quiescent state are stimulated to proliferate and restore the BM; self-renewal of HSCs is involved in this process.[1] In a mouse experimental model, only one HSC was found to be sufficient to reconstitute the entire hematopoiesis.[2] In this system, it has been suggested that daughter cells derived from HSCs can either commit to a program of differentiation that will eventually result in production of mature, nonproliferating cells or retain HSC properties.

Several proteins thought to be involved in HSCs for induction of self-renewal, including Wnt and Notch ligand families, have been isolated[3-5]; however, what lies downstream of them in the signaling pathway, especially molecules involved in DNA replication, is not known.

PSF1 (partner of SLD5-1) is evolutionarily conserved and is involved in DNA replication in lower eukaryotes,[6-8] and human.[9] PSF1 forms a tetrameric complex (GINS complex) with SLD5, PSF2, and PSF3. Recently, crystal structure of the human GINS complex was reported.[10-13] In yeast, GINS complex associates with MCM2-7 complex and CDC45, and this C-M-G complex (CDC45-MCM2-7-GINS) regulates both the initiation and progression of DNA replication.[14-17]

Previously, we cloned the mouse ortholog of *PSF1* from an HSC-specific cDNA library.[18] *PSF1* is predominantly expressed in highly proliferative tissues, such as testis and BM. Loss of *PSF1* causes embryonic lethality around the implantation stage.[18] *PSF1*$^{-/-}$ embryos revealed impaired proliferation of multipotent stem cells, ie, the inner cell mass. In mice, *PSF1* is highly expressed in proliferating HSCs and the hematopoietic progenitor cells (HPCs). However, the biologic function of PSF1 in hematopoiesis is not understood.

In this study, we used *PSF1*$^{+/-}$ mice for studying the function of PSF1 in hematopoiesis. Here we show that haploinsufficiency of *PSF1* causes loss of regeneration capacity resulting from a delay in induction of acute proliferation of HSCs after BM ablation. Our data suggest that both alleles of *PSF1* are essential for acute proliferation of HSCs after BM ablation.

Methods

Mice

C57BL/6 mice were purchased from SLC (Shizuoka, Japan). *PSF1* mutant mice and *Runx1*-deficient mice (*Runx1*-deficient mice were a gift from Dr T. Watanabe, Tohoku University, Sendai, Japan) were maintained and bred as described.[18,19] All animal studies were approved by the Animal Care Committee of Kanazawa University and the Osaka University Animal Care and Use Committee. For BM ablation studies, 8-week-old wild-type and *PSF1*$^{+/-}$ mice were treated with a single tail vein injection of 5-fluorouracil (5-FU; 150 mg/kg body weight; Kyowa Hakko Kogyo, Tokyo, Japan).

Immunohistochemistry and FACS analysis

Tissue fixation, preparation of tissue sections, and staining of sections with antibodies were performed as described previously.[18] For immunohistochemistry of fetal liver (FL), rabbit anti-PSF1 antibody was used.[18] Horseradish

Submitted January 29, 2008; accepted September 7, 2008. Prepublished online as *Blood* First Edition paper, November 4, 2008; DOI 10.1182/blood-2008-01-136879.

The online version of this article contains a data supplement.

The publication costs of this article were defrayed in part by page charge payment. Therefore, and solely to indicate this fact, this article is hereby marked "advertisement" in accordance with 18 USC section 1734.

peroxidase-conjugated secondary antibodies were obtained from Jackson ImmunoResearch Laboratories (West Grove, PA). For immunocytochemistry, we used monoclonal anti-PSF1 antibody (Aho57.2; see next paragraph below) as a first antibody and Alexa 488–conjugated antirat IgG (Invitrogen, Carlsbad, CA) as a second antibody. Stained cells and the sections were observed using an Olympus IX-70 microscope equipped with UPlanFI 4/0.13 and LCPlanFI 20 /0.04 dry objective lenses (Olympus, Tokyo, Japan). Images were acquired with a CoolSnap digital camera (Roper Scientific, Trenton, NJ), and processed with Adobe Photoshop version 8.0.1 software (Adobe Systems, San Jose, CA).

For the generation of monoclonal anti-PSF1 antibodies, cDNA encoding the full-length protein sequence of PSF1 was amplified by polymerase chain reaction (PCR), and then cDNA was ligated into pGEX-4T-1 vector (GE Healthcare, Little Chalfont, United Kingdom) for the preparation of glutathione S-transferase (GST)–fusion proteins. PSF1-coding region was amplified from the mouse NIH3T3 cDNA using the primers 5′-GGA ATT CAT GTT CTG CGA AAA AGC TAT G-3′ (sense) and 5′-GGA ATT CTC AGG ACA GCA CGT GCT CTA GA-3′ (antisense) and was subsequently subcloned as a *Eco*RI-*Eco*RI fragment into the pGEX-4T-1 vector (GE Healthcare) in the correct reading frame to express the GST-PSF1 fusion protein. This construct was transformed into *Escherichia coli* JM109 strains (Toyobo Engineering, Osaka, Japan) to obtain GST-tagged fusion proteins. Recombinant GST-PSF1 was purified using glutathione-Sepharose 4B column (GE Healthcare) according to the manufacturer's instructions. Purified GST-fused proteins were used as antigen for immunization of rats, and rat/mouse hybridomas were established by standard procedures.[20] A stable hybridoma cell line, aho57.2, was obtained. The specificities of all antibodies were determined by immunoblotting and immunocytochemistry.

Preparation of FL and BM cells and fluorescence-activated cell sorter (FACS) analysis was as described previously.[21,22] The antibodies used in flow cytometric analysis for lineage marker (Lin) were fluorescein isothiocyanate– or phycoerythrin-conjugated Gr-1 (RB6-8C5), Mac-1 (M1/70), B220 (RA3-6B2), TER119, anti-CD4 (GK1.5), and anti-CD8 (53-6.72). Allophycocyanin-conjugated anti–c-kit (ACK2), and biotin-conjugated anti–Sca-1 and CD34 were also applied. Biotinylated anti–Sca-1 or CD34 was visualized with peridinin chlorophyll protein–streptavidin. These antibodies were purchased from BD Biosciences (San Jose, CA). The stained cells were analyzed by FACSCalibur (BD Biosciences) and sorted by JSAN (Bay Bioscience, Kobe, Japan). For immunocytochemistry of HSCs from 5-FU–treated BM, 300 $CD34^+$ KSL cells were isolated by sorting from BM obtained from 5 mice 4 days after 5-FU treatment. The average number of total BM mononuclear cells and $CD34^+$ KSL obtained from right and left femurs and tibias after treatment with 5-FU was 9.3 plus or minus 5.3 × 10^6 and 60 plus or minus 38, respectively.

For the analysis of apoptosis, cells were stained with anti–annexin V antibodies (eBioscience, San Diego, CA). For platelet analysis, blood from wild-type and mutant mice was obtained from the tail vein and collected in phosphate-buffered saline (PBS) containing 3.8 mM citric acid, 7.5 mM trisodium citrate, and 10 mM of dextrose (PBS–acid-citrate-dextrose). Cells were stained with fluorescein isothiocyanate–conjugated anti-CD41 antibody (eBioscience).

qRT-PCR

Total RNA was isolated using the RNAeasy Kit (QIAGEN, Valencia, CA) according to the manufacturer's instructions. RNA was reverse transcribed using the ExScript RT Reagent Kit (Takara, Kyoto, Japan). Quantitative reverse-transcription polymerase chain reaction (qRT-PCR) was performed using Platinum SYBR Green qPCR SuperMix-UDG (Invitrogen) on an Mx3000 system (Stratagene, La Jolla, CA). Levels of the specific amplified cDNAs were normalized to the level of glyceraldehydes-3-phosphate dehydrogenase (*GAPDH*) housekeeping control cDNA. We used the following primer sets: 5′-GAA GGG CTC ATG ACC ACA GT-3′ and 5′-GGA TGC AGG GAT GAT GTT CT-3′, for *GAPDH*, and 5′-CCG GTT GCT TCG GAT TAG AG-3′ and 5′-CTC CCA GCG ACC TCA TGT AA-3′ for *PSF1*.

Cell culture

The colony formation unit in culture (CFU-c) assay was performed as described previously.[21] A total of 2 × 10^2 KSL-Mac-$1^{-/lo}$ cells that had been sorted from the BM of wild-type or $PSF1^{+/-}$ mice were placed in 1 mL semisolid medium (MethoCult; StemCell Technologies, Vancouver, BC). After 10 days of culture, the number of colonies was counted.

For the analysis of sensitivity of HSCs to 5-FU, 10^3 KSL cells derived from wild-type or $PSF1^{+/-}$ mice were seeded onto semisolid medium and continuously cultured for 10 days with or without 5-FU (1 ng/mL to 1 μg/mL). Each condition was represented by at least 3 wells, and each experiment was performed in triplicate. To examine the number of apoptotic cells in the population of colony-forming cells, colonies grown in methylcellulose semisolid medium were harvested 6 days after the CFU-c assay was initiated, and the cells were stained with Cy5-conjugated anti–annexin V antibody (eBioscience).

Cell-cycle analysis

Cells were sorted by FACS and fixed in 70% ethanol overnight. After treatment with RNase A (0.5 mg/mL; Sigma-Aldrich, St Louis, MO), cells were labeled with 5 μg/mL propidium iodide (PI) and analyzed by FACSCalibur.

Transfection and immunoblot analysis

NIH3T3 cells were transfected with pEF-BOSE, pEF-flag-PSF1, pEF-Myc-SLD5, pEF-HA-PSF2, and/or pEF-VSVG-PSF3, and immunoblotting was performed as previously described.[23] GAPDH was detected with anti-GAPDH antibodies (Chemicon International, Temecula, CA) for endogenous protein control. Transfection efficiency of each plasmid was determined by qRT-PCR (see "qRT-PCR"). We used the following primer sets: 5′-ATG GAC TAC AAG GAC GAC GAT GAC-3′ and 5′-CTC CCA GCG ACC TCA TGT AA-3′ (for *FLAG-PSF1*); 5′-GAG ATG AAC CGA CTT GGA AAG GG-3′ and 5′-TCC TCA TCA CGC ATC TGT TC-3′ (for *VSVG-PSF2*); 5′-TAC GAT GTT CCA GAT TAC GCG GG-3′ and 5′-CAG GAT GTC GTC CAA AGA CA-3′ (for *HA-PSF3*); 5′-CTC ATC TCA GAA GAG GAT CTG GG-3′ and 5′-GTG TGG TCC ATA TAC TCT TTG-3′ (for *Myc-SLD5*).

Transplantation study

For the analysis of sensitivity of HSCs to 5-FU in vivo, 8-week-old mice were treated with 5-FU (see "Cell culture"), and after 1 day of 5-FU treatment, $PSF1^{+/+}$ or $PSF1^{+/-}$ BM mononuclear cells (Ly5.2, 4 × 10^5) were transplanted into lethally irradiated (8.5 Gy) recipients (Ly5.1) together with untreated normal Ly5.1 BM cells (2 × 10^5). Four weeks after transplantation, donor contribution was determined by FACS using anti-Ly5.1 (eBioscience) and anti-Lin antibodies mixture.

Results

PSF1 is predominantly expressed in proliferating immature hematopoietic cells

Previously, we reported that *PSF1* expression was predominantly observed in immature cell populations in embryonic and adult tissues, such as blastocysts and spermatogonium in the adult.[18] Moreover, *PSF1* expression was observed in immature hematopoietic cells (HCs) designated as Lin^- $c\text{-}kit^+$ $Sca\text{-}1^+$ (KSL) at the RNA expression level. To confirm whether PSF1 protein is expressed in HSCs or not, $CD34^-$ or $CD34^+$ KSL, $Lin^-c\text{-}kit^+Sca\text{-}1^-$ (KL) or Lin^+ cells from adult BM were sorted, and expression of PSF1 was determined in each fraction (Figure 1A). It has been reported that $CD34^-$ KSL cells in the adult mouse BM are dormant and represent HSCs with long-term marrow repopulating ability, whereas $CD34^+$ KSL cells are progenitors with short-term

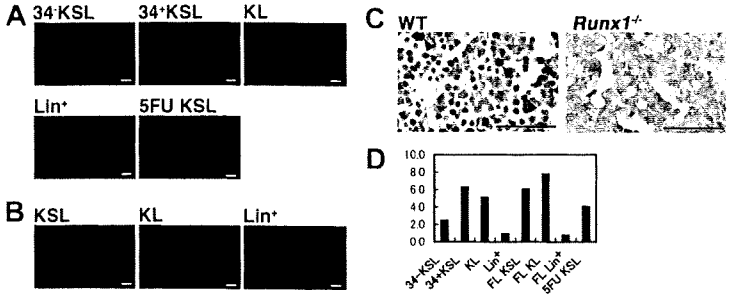

Figure 1. PSF1 expression in proliferating HSC population. (A,B) Immunostaining of several BM (A) or FL-derived (B) HC population with anti-PSF1 antibody. (A) CD34$^-$KSL (CD34$^-$c-kit$^+$Sca-1$^+$Lin$^-$ cells), 34$^+$KSL (CD34$^+$c-kit$^+$Sca-1$^+$Lin$^-$ cells), KL (c-kit$^+$Sca-1$^-$Lin$^-$ cells), Lin$^+$ (Lin$^+$ cells), and 5-FU KSL (5-FU-treated mouse derived CD34$^+$KSL cells). (B) KSL (c-kit$^+$Sca-1$^+$Lin$^-$ cells), KL (c-kit$^+$Sca-1$^-$Lin$^-$ cells), and Lin$^+$ (Lin$^+$ cells). Green color shows PSF1 staining. Nuclei were counterstained with PI (red). Bar represents 10 μm. (C) Sections of E12.5 FL from wild-type (WT) or *Runx1*$^{-/-}$ mice were stained with anti-PSF1 polyclonal antibody. Sections were counterstained with hematoxylin (original magnification ×400). Arrows indicate PSF1$^+$ cells. Bars represent 50 μm. (D) *PSF1* mRNA expression in various HC fractions of BM or FL cells as indicated in panel A. 5-FU KSL indicates KSL cells were sorted from BM of mice 4 days after treatment with 5-FU. The values were normalized to the amount of mRNA in Lin$^+$ cells from BM.

reconstitution capacity.[2,24] In the steady state, a high level of PSF1 expression was observed in CD34$^+$ KSL cells and KL cells, whereas a very low level of PSF1 expression was observed in CD34$^-$ KSL cells. However, no PSF1 expression was detected in mature cells (Lin$^+$; Figure 1A). It was reported that, after BM ablation, all HSCs express CD34 in a situation when BM is acutely reconstituted.[25] Therefore, to know whether PSF1 expression in HSCs correlates with cell cycle of HSCs, CD34$^+$ KSL cells were sorted from the BM 4 days after ablation of the BM by 5-FU. As expected, almost all CD34$^+$ KSL cells were stained by anti-PSF1 antibody (Figure 1A).

It is known that HSCs in the FL contain cells that cycle at a higher rate than those in the adult BM and HSCs express the Mac-1 antigen.[26] We sorted KSL (without Mac-1), KL, and Lin$^+$ cells from the FL at embryonic day (E) 12.5 and determined PSF1 expression. High PSF1 expression was found in both KSL and KL cells (Figure 1B), and Lin$^+$ cells did not express PSF1 as seen in the adult BM.

On immunohistochemistry, PSF1 expression was seen in a small population of round HCs in the FL at E12.5 (Figure 1C). However, in the adult liver, which is no longer a hematopoietic organ, PSF1 expression was not observed (data not shown). Furthermore, to test the specificity of this staining in the FL, we studied PSF1 expression in *Runx1*-deficient mice, which lack definitive hematopoiesis[27] and could not detect PSF1-positive cells in the FL in this mutant embryo (Figure 1C). To confirm the specific expression of PSF1 in proliferative and immature HCs, we performed qRT-PCR (Figure 1D). PSF1 was highly expressed in BM-derived CD34$^+$ KSL and Lin$^-$Kit$^+$, and FL-derived Lin$^-$Kit$^+$Sca1$^+$ and Lin$^-$Kit$^+$ cells. KSL cells derived from BM at 4 day after 5-FU treatment also expressed higher amounts of *PSF1* transcript than CD34$^-$ KSL cells. These results demonstrated that PSF1 is highly expressed in proliferating HSCs and progenitors.

Pool size of HSCs/HPCs is decreased in *PSF1*$^{+/-}$ old mice

To investigate how haploinsufficiency of *PSF1* affects hematopoiesis, we analyzed the BM of *PSF1*$^{+/-}$ mice.[18] Although no significant differences were found in KSL cells (Figure 2A) and mature cells populations (data not shown) between wild-type and *PSF1*$^{+/-}$ at 8 weeks of age, the relative number of KSL cells was approximately 2-fold lower in one year-old mice compared with wild-type littermates (Figure 2B). In addition, the population of CD34$^-$ KSL cells (LT-HSCs), CD34$^+$ KSL cells (KSL: ST-HSCs),

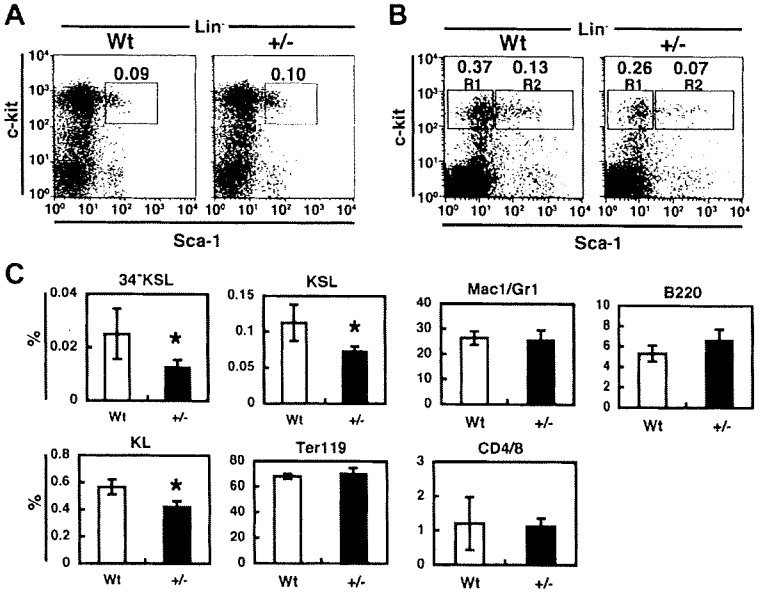

Figure 2. Haploinsufficiency of *PSF1* for hematopoiesis. (A,B) Cells of KSL populations in the BM from 8-week-old mice (A) and 1-year-old mice (B) were analyzed. Percentage of each fraction indicated by box was represented. R1 and R2 in panel B indicates fraction from c-kit$^+$Sca-1$^-$Lin$^-$ cells and c-kit$^+$Sca-1$^+$Lin$^-$ cells, respectively. (C) Quantitative evaluation in percentage of each fraction among all BM cells of 1-year-old wild-type (Wt) or *PSF1*$^{+/-}$ (+/−) mice as indicated. Mac-1/Gr-1 (myeloid), B220 (B cells), CD4/CD8 (T cells), or TER119 (erythroid). HSCs populations were studied in a CD34$^-$ KSL cell population. Populations of KSL (c-kit$^+$Sca-1$^+$Lin$^-$ cells) and KL (c-kit$^+$Sca-1$^-$Lin$^-$ cells) were also evaluated. *$P < .05$.

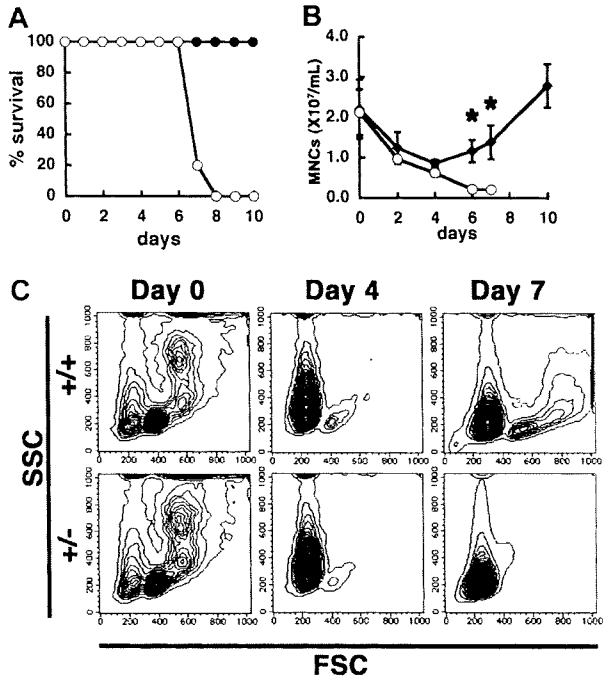

Figure 3. Hypersensitivity of *PSF1*$^{+/-}$ mice to 5-FU. (A) Survival curves after 5-FU injection. ○ indicate *PSF1*$^{+/-}$ 8-week-old mice (n = 10); and ●, wild-type 8-week-old mice (n = 10). (B) Number of mononuclear cells in the peripheral blood of wild-type (●) and *PSF1*$^{+/-}$ (○) mice over time after 5-FU injection. 5-FU was injected into 8-week-old mice on day 0. Means plus or minus SEM are shown (n = 10). *$P < .05$ vs those in PSF1$^{+/-}$ mice on days 2, 4, 6, 8, and 10 after BM ablation with 5-FU. (C) Kinetics of BM cells after 5-FU injection. +/+ indicates wild-type mice; and +/−, *PSF1*$^{+/-}$ mice. Results of FACS analysis are shown. SSC indicates side-scattered light; and FSC, forward-scattered light. Blue represents RBC; and red, leukocytes.

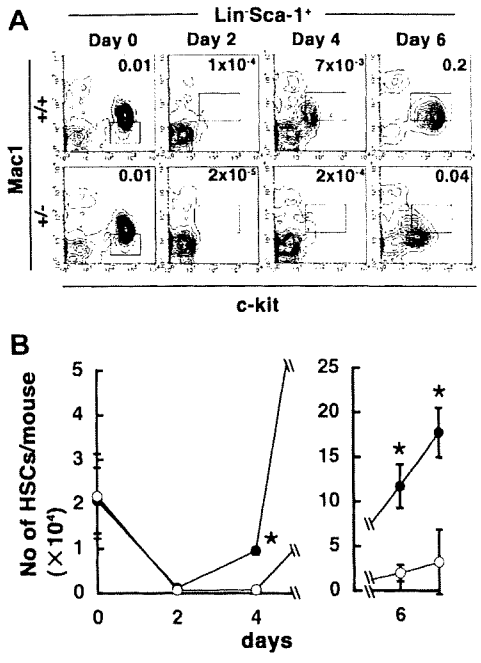

Figure 4. Both alleles of *PSF1* are required for acute reconstitution after BM ablation. (A) Time course of c-kit and Mac-1 expression in Lin$^-$Sca-1$^+$ cells during BM reconstitution after 5-FU injection (+/+, 8-week-old wild-type mice; +/−, 8-week-old *PSF1*$^{+/-}$ mice). Results of FACS analysis are shown. Boxes indicate HSC-containing populations. Percentage of all BM cells corresponding to HSC population indicated by the box is shown in the right corner of each figure. (B) Total number of KSL cells derived from the femurs and tibias of wild-type (●) and *PSF1*$^{+/-}$ mice (○) on the indicated days before (day 0) and after 5-FU injection as described in panel A. *$P < .05$ versus that in *PSF1*$^{+/-}$ mice on the respective day.

and c-kit$^+$Sca-1$^-$Lin$^-$ (KL) were significantly decreased in *PSF1*$^{+/-}$ mice (Figure 2C). The relative cell number of each type of mature HC such as myeloid cells (Mac1/Gr-1$^+$ cells), T cells (CD4/CD8 cells), B cells (B220$^+$), or erythroid cells (TER119$^+$) of the *PSF1*$^{+/-}$ BM was similar to that of the wild-type BM (Figure 2C). These data suggested that both alleles of *PSF1* gene are essential for maintenance of the proper pool size of HSCs or HPCs throughout life.

PSF1$^{+/-}$ mice show hypersensitivity for fluorouracil in the BM

Next, we ablated the BM by 5-FU injection, which kills cycling HSCs/HPCs and forces dormant HSCs into cycle, and studied the ability of *PSF1*$^{+/-}$ mice to reconstitute BM hematopoiesis and analyzed the effect of haploinsufficiency of *PSF1* on HSCs and HPCs (Figure 3A). Although the LD_{50} of 5-FU is 350 mg/kg in normal mice,[28] the *PSF1*$^{+/-}$ mice died within 8 days after a single injection with a lower dose 5-FU (150 mg/kg), whereas wild-type mice did not die with this treatment. On 5-FU injection in *PSF1*$^{+/-}$ mice, the number of peripheral leukocytes decreased precipitously over 7 days; however, in wild-type mice, the number of peripheral leukocytes decreased over 4 days and then it began to increase by day 6 (Figure 3B). After 5-FU injection, the forward scatter$^{dull/high}$ population, which includes lymphocytes, granulocytes, and monocytes, were reconstituted in the BM of wild-type mice after approximately day 7; however, such reconstitution was not observed in the BM of *PSF1*$^{+/-}$ mice (Figure 3C red-colored population). We also calculated the number of peripheral red blood cells and platelets; however, no significant differences were found between *PSF1*$^{+/+}$ and *PSF1*$^{+/-}$ mice in normal and acute phase (data not shown).

PSF1 is essential for HSC proliferation after 5-FU treatment

Before 5-FU injection, there were no obvious differences in the numbers of HSCs and HPCs in the BM between 8-week-old wild-type and *PSF1*$^{+/-}$ mice (Figures 2A, 4A). 5-FU injection induces HSCs into cycle, and it was reported that these cycling HSCs weakly express Mac-1.[26,29] We therefore studied whether 5-FU injection promotes the proliferation of Mac-1^{lo}–expressing HSCs. Before 5-FU injection, the number of HSC population designated as Mac-1$^-$ KSL was not significantly different between wild-type and *PSF1*$^{+/-}$ mice as shown in Figure 2A (see also Figure 4A,B). After 5-FU injection, the KSL cell population decreased in both wild-type and *PSF1*$^{+/-}$ mice during the first few days (Figure 4A). Four to 6 days after 5-FU injection, the population of cycling Mac-1^{lo}–KSL cells increased dramatically in wild-type mice, whereas very few of the KSL cells except for the Mac-1^{lo}–KSL population appeared in the *PSF1*$^{+/-}$ mice (Figure 4A). Because of this delay of recovery, the absolute number of HSCs in the BM was approximately 5.9-fold lower in *PSF1*$^{+/-}$ mice compared with that in wild-type mice at 6 days after 5-FU treatment (Figure 4B).

Loss of PSF1 leads to delayed HSC proliferation in the acute phase after BM ablation

Because it has been reported that the percentage of proliferating HSCs reaches a maximum on approximately day 6 in normal mice,[29] we sorted the total population of HSCs (KSL–Mac-1$^{-/lo}$) and HPCs (Lin$^-$Sca-1$^-$c-kit$^+$Mac-1$^{-/lo}$) on day 6 after 5-FU

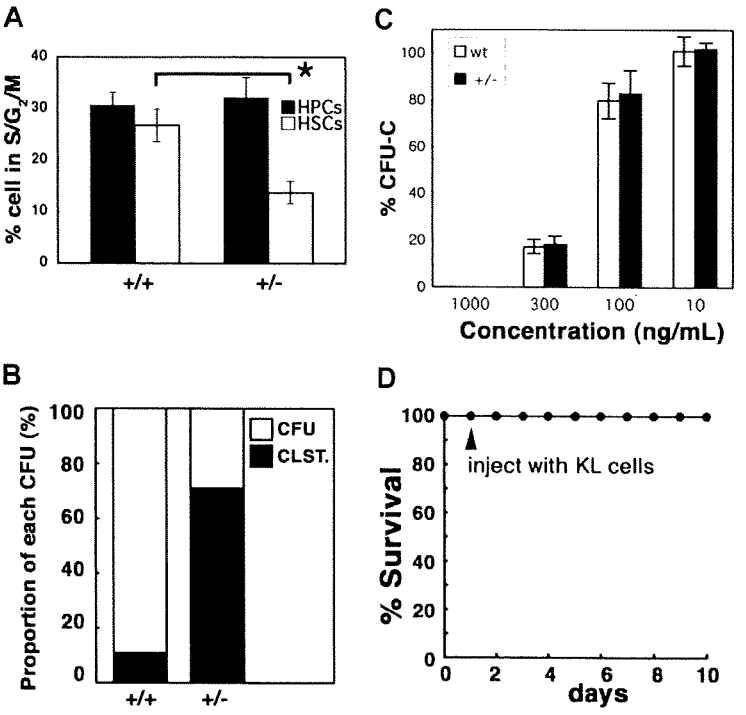

Figure 5. Loss of PSF1 leads to delay of HSC proliferation in the acute phase. (A) Percentage of KSL cells or HPCs ($Lin^-c\text{-}kit^+Sca\text{-}1^-$) in the $S/G_2/M$ phase among the total number of HSCs or HPCs, respectively, on day 6 after 5-FU injection as described in Figure 4A. ■ indicates HPCs; □, KSL cells. Mean values plus or minus SEM are shown (n = 5). $^*P < .05$. (B) CFU-c assay using KSL cells obtained from mice on day 6 after 5-FU injection. +/+ indicates wild-type mice; and +/−, *PSF1*$^{+/-}$ mice. ■ indicates CFU cluster (CLST; containing < 30 cells); □, CFU-C (CFU; containing > 30 cells). (C) Comparison between wild-type and *PSF1*$^{+/-}$ KSL cells for sensitivity to 5-FU toxicity. Sorted KSL cells from the BM of 8-week-old mice were seeded in semisolid medium with indicated concentration of 5-FU, and total CFU-C number was counted after 10 days of culturing. Results are expressed as a percentage compared with control condition (100%). (D) Rescue experiments. *PSF1*$^{+/-}$ mice were injected with 5-FU on day 0. One day after 5-FU injection (▲), $Lin^-CD45^+c\text{-}kit^+$ cells (KL cells; 5×10^4/mice) that had been derived from wild-type BM were injected into *PSF1*$^{+/-}$ mice (n = 5).

injection and analyzed the cell cycle of those HSCs and HPCs. The cells were analyzed for DNA content by PI staining (Figure 5A). The percentage of HSCs in the $S/G_2/M$ phase was approximately 50% lower in *PSF1*$^{+/-}$ mice than those in wild-type mice, whereas the percentage of HPCs in the $S/G_2/M$ phase was not significantly different between *PSF1*$^{+/-}$ and wild-type mice. These data suggest that both alleles of *PSF1* are essential for acute BM reconstitution.

When HSCs are cultured in semisolid media, they divide and generate large colonies, including mature HCs. If *PSF1* haploinsufficiency leads to cell death in HSCs, HSCs cannot form colonies in vitro. Therefore, next we investigated the in vitro colony-forming capacity of HSCs ($KSL\text{-}Mac\text{-}1^{-/lo}$) that had been obtained on day 6 after 5-FU injection by cell sorting (Figure 5B). The HSCs from *PSF1*$^{+/+}$ and *PSF1*$^{+/-}$ mice formed the same total numbers of colonies and clusters (data not shown); however, the HSCs from *PSF1*$^{+/-}$ mice formed a markedly higher number of CFU clusters (> 30 cells) compared with *PSF1*$^{+/+}$ cells. In the case of HSCs derived from wild-type mice, approximately 89% of all colonies were large colonies; however, approximately 71% of colonies generated by HSCs from *PSF1*$^{+/-}$ mice were small colonies. To determine whether haploinsufficiency of *PSF1* simply induced cell death resulting in reduced colony size in CFU-c assay, we examined the number of apoptotic cells in the colony-forming cell population by staining with anti–annexin V antibodies (Table 1). No significant differences were found in the apoptotic cells with respect to Lin^-Kit^+, Lin^-Sca1^+, and Lin^- population between cells from CFU-c derived from *PSF1*$^{+/+}$ and *PSF1*$^{+/-}$ HSCs. These data suggested that the decreased colony size in *PSF1*$^{+/-}$ CFU-c is not induced by activation of DNA damage checkpoint and cell death. These results indicated that *PSF1*$^{+/-}$ HSCs may not easily divide into daughter cells committed to a program of differentiation, but haploinsufficiency did not induce cell death. Furthermore, to test the possibility that *PSF1*$^{+/-}$ HSCs are simply more sensitive to 5-FU toxicity, KSL cells were sorted from BM of wild-type or *PSF1*$^{+/-}$ mice and seeded onto semisolid medium in the presence or absence of 5-FU. Figure 5C illustrates the effect of exposure to various concentrations of 5-FU on colony-forming activity of KSL cells. KSL cells survived and those from wild-type and *PSF1*$^{+/-}$ formed comparable number of colonies, suggesting that deletion of one *PSF1* allele of HSCs does not cause hypersensitivity for 5-FU. To support this interpretation, BM of wild-type or *PSF1*$^{+/-}$ mice was collected after 1 day of 5-FU treatment and transplanted into lethally irradiated recipient mice together with untreated normal cells as competitor. After 4 weeks of transplantation, donor contribution was determined by FACS. The percentage of contributed cells (chimerism) was 56 plus or minus 12 and 24 plus or minus 14 in recipients, which were transplanted with wild-type or *PSF1*$^{+/-}$ BM cells, respectively, although the contribution of PSF1$^{+/-}$-derived HSCs in recipient mice was slightly less. These data suggested that deletion of one *PSF1* allele of HSCs does not cause hypersensitivity for 5-FU. Moreover, transplantation of HSCs and HPCs that had been obtained from wild-type mice completely rescued the lethality of 5-FU in *PSF1*$^{+/-}$ mice (Figure 5D). These data suggest that the defect in acute reconstitution of the BM in *PSF1*$^{+/-}$ mice is not caused by disruption of the BM microenvironment in these mice.

Table 1. Percentage of apoptotic cells among CFU-c cell population

Marker	Genotype	
	PSF1$^{+/+}$	PSF1$^{+/-}$
Lin^-Kit^+	39 ± 33	36 ± 29
Lin^-Sca1^+	3.6 ± 2.3	2.6 ± 1.6
Lin^-	2.2 ± 1.1	1.8 ± 1.4

It was reported that PSF1 is essential for DNA replication in yeast.[14-17] This observation raises the possibility that haploinsufficiency of *PSF1* leads to abnormal DNA replication, activation of DNA damage checkpoint, S-phase arrest, and cell death in mice. To evaluate this possibility, apoptotic cells were quantified by FACS analysis after staining with annexin V in 5-FU–treated or untreated BM cells (Table 2). In *PSF1*$^{+/-}$ BM cells, apoptotic cells from Lin^-, Lin^-Kit^+, or $Lin^-Kit^+Sca^+$ cell populations were slightly

Table 2. Percentage of apoptotic cells in various hematopoietic cell populations

Marker	Genotype	
	$PSF1^{+/+}$	$PSF1^{+/-}$
Normal state		
$Lin^-Kit^+Sca1^+$	5.4 ± 4	9.3 ± 0.4
Lin^-Kit^+	4.5 ± 3	8.1 ± 0.2
Lin^-	7.0 ± 5	12 ± 0.6
5-FU treated*		
$Lin^-Kit^+Sca1^+$	5.2 ± 2	7.4 ± 0.5
Lin^-Kit^+	4.2 ± 2	5.1 ± 0.7
Lin^-	4.7 ± 2	5.9 ± 1

*BM cells were collected from mice 6 days after treatment with 5-FU.

increased compared with the analogous populations derived from wild-type mice; however, none of these differences was statistically significant. In addition, no obvious S-phase arrest was found in $PSF1^{+/-}$ HSCs (Figure 5A). We also examined the expression of ATM, ATR, XCCR1, Brca2, and p21 in both wild-type and $PSF1^{+/-}$ CD34-KSL cells by qRT-PCR; however, no obvious differences were found (data not shown). These data suggested that haploinsufficiency does not lead to abnormal DNA replication or increased activation of DNA damage checkpoint.

Taken together, these data indicate that both alleles of *PSF1* are essential for promoting HSC cycling and that this requirement is limited to HSCs.

PSF1 regulates molecular stability of other GINS components in mutual manner

To address whether the silencing of one of the GINS components, PSF1, affects the cellular stability of other GINS components, we performed ectopic expression of all GINS component with or without PSF1 (Figure 6). For the evaluation of the transfection efficiency by plasmids, the amounts of overexpressed gene transcripts were quantified by real-time PCR; no significant differences were found between GINS and G-NS condition for VSVG-PSF2, HA-PSF3, and Myc-SLD5 expression (Table 3). These data indicated that transfection efficiencies of all plasmids were almost equivalent between GINS and G-NS conditions. When all GINS components (PSF1, PSF2, PSF3, and SLD5) were cotransfected, a stable "GINS" complex was formed. However, lack of PSF1 led to destabilization of PSF2, PSF3, and SLD5 (G-NS; Figure 6A). These data suggest that lack of PSF1 results in the formation of an

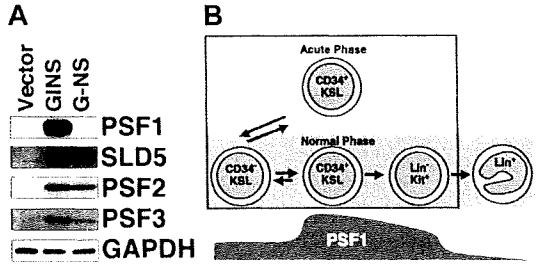

Figure 6. PSF1 mutually regulates molecular stability of other GINS components. (A) Western blot analysis of GINS components ectopically expressed on NIH3T3 cells. Cells were cotransfected with VSVG-PSF2, HA-PSF3, and Myc-SLD5 in the presence (GINS) or absence (G-NS) of Flag-PSF1 or empty vector (Vector). The blots were probed with specific antibodies as indicated. GAPDH was used as a loading control. (B) Scheme of PSF1 expression in the course of HSC differentiation. The level of PSF1 expression is represented by the dark gray area. Both alleles of *PSF1* are essential for populations in the light gray area.

Table 3. Relative mRNA expression in transfected cells

Average of relative expression	Plasmid used for transfection	
	Flag-PSF1, VSVG-PSF2, HA-PSF3, Myc-SLD5 (GINS)	VSVG-PSF2, HA-PSF3, Myc-SLD5 (G-NS)
VSVG-PSF2	1	1.05
HA-PSF3	1	1.14
Myc-SLD5	1	1.14

incomplete GINS complex, along with the destabilization of other GINS components in $PSF1^{+/-}$ HSCs. Finally, we concluded that PSF1 is expressed in proliferating HSCs and is essential for BM regeneration and regulation of stem cell pool size (Figure 6B).

Discussion

In this study, we showed that PSF1 is highly expressed in proliferating HSCs, and haploinsufficiency of *PSF1* caused severe delay in induction of HSC proliferation during ablated BM reconstitution and disrupted pool size maintenance of HSCs throughout life. In addition, we showed that PSF1 regulates protein stability of other GINS components.

During embryogenesis, $PSF1^{-/-}$ embryos show severe growth defect in the inner cell mass, that is, the pluripotent stem cells.[18] This observation raises the possibility that PSF1 could regulate the proliferation and/or pool size for other tissue stem cells. Recently, stem cells were identified in the small intestine.[30] Crypt base columnar cells are stem cells and can be visualized by continuous bromodeoxyuridine incorporation study. Our preliminary experiment showed that the number of crypt base columnar cells also decreased in adult $PSF1^{+/-}$ mice compared with adult wild-type mice (Figure S1, available on the *Blood* website; see the Supplemental Materials link at the top of the online article). Further experiments may help establish the function of PSF1 in the regulation of cell proliferation and/or the pool size of various tissue stem cells.

So far, a multiplicity of molecules have been studied for their role in cell-cycle progression, including extrinsic factors, such as Notch and sonic hedgehog, Wnt3a, etc, and intrinsic factors, such as Bmi1, PTEN, p21, p18, and others.[31] However, the mechanism of DNA replication in HSCs has not been elucidated. Although the essential role of PSF1 in DNA replication has been reported in yeast,[8] its function in mammalian cells has not been clearly understood. We previously reported that *PSF1* was essential for cell division of totipotential embryonic stem cells by gene-targeting studies and showed that *PSF1* was highly expressed in adulthood in BM, testis, and ovary, where cell division of stem cells is actively induced in the adult. Here we reported that PSF1 is essential for acute proliferation of HSCs. Taken together, it is clear that PSF1 plays important roles in cell proliferation of the stem cell system. Moreover, we and other groups isolated mammalian PSF2, PSF3, and SLD5, which together make up the GINS complex, and the roles of these GINS component have been reported in cell division.[7,8] In this report, we found that PSF1 expression was weak in slow cycling $CD34^-$ LT-HSCs and high in cycling $CD34^+$ ST-HSC. Therefore, the GINS complex is likely to closely associate with cell cycle of HSCs. At present, molecules affecting PSF1 expression in dormant HSCs have not been isolated; however, proliferating HSCs after BM ablation by 5-FU almost exclusively express PSF1 at high levels. This suggested that PSF1 expression is

inductively, but not intrinsically, regulated in HSCs affected by exogenous molecules produced from cells responding to BM suppression. At present, although it is not clear whether PSF1 plays a role in DNA replication of HSCs, isolation of molecules affecting PSF1 expression in HSCs may contribute to the understanding of process of self-renewal in HSCs.

It was reported that "GINS" replication complex, which is composed of PSF1, PSF2, PSF3, and SLD5, interacts with CDC45 and MCM complex and is involved in the initiation of DNA replication in lower eukaryote.[14-17] To determine whether haploinsufficiency of *PSF1* impairs DNA replication at stem cell level resulting in reduced pool size of HSCs, we examined the expression levels of DNA-damage checkpoint genes, such as ATM, ATR, XCCR1, BRCA2, and p21 in HSCs. No significant differences were found between $CD34^-$ KSL cells derived from young and old $PSF1^{+/+}$ and $PSF1^{+/-}$ BM (data not shown). These data suggested that the decreased pool size of HSC population in $PSF1^{+/-}$ BM is not induced by activation of DNA damage checkpoint.

In this study, haploinsufficiency of PSF1 severely suppressed BM reconstitution by delaying the proliferation of the HSC population. Based on our result, there are 2 possibilities to explain this suppression not only by gene-dose effect, but also other processes. As one possibility, PSF1 may bring about the molecular stability of DNA replication proteins. Overexpression studies suggested that PSF1 regulates stable expression of other GINS components (Figure 6A). Thus, it is probable that lower expression of PSF1 in HSCs of $PSF1^{+/-}$ mice may lead to down-regulation of SLD5, PSF2, and PSF3 in HSCs. Therefore, incompletely formed GINS complex may have a dominant negative effect and/or induce instability of other DNA replication complexes, such as CDC45 or MCMs. Another possibility is that PSF1 may induce HSC specific gene expression for effective engraftment capacity. It was reported that HSCs shift gene expression and engraftment phenotype with cell cycle transit.[32] Compared with HSCs from wild-type mice, HSCs obtained from 5-FU-injected $PSF1^{+/-}$ mice expressed a lower level of Mac-1, which appeared to be expressed in cycling stem cells and to be involved in cell adhesion (Figure 5A).[26] Thus, haploinsufficiency of *PSF1* may affect HSC properties. As it is thought that DNA replication of important genes for cell function occurs in the early period of the S phase, it is possible that PSF1 regulates the expression of several genes involved in the formation of the BM stem cell niche through DNA replication specifically in HSCs. In addition, loss of PSF1 causes abnormality of chromatin segregation in mice and nematodes (M.U., N.T., unpublished data, May 1, 2007). It has been also reported that PSF2 depletion inhibits the transition of metaphase to anaphase through the suppression of the attachment of tubulin to the kinetochore.[33] These data suggest that the GINS complex might have roles in other biologic processes.

It is also known that, after chemotherapy with anticancer drug, some patients have prolonged BM suppression for unknown reasons.[34] Moreover, BM dysfunction resulting in pancytopenia is observed with aging in elderly people for unknown reasons. Haploinsufficiency of *PSF1* in mice induced delay of BM recovery after 5-FU treatment and attenuated the number of HSCs with aging. Therefore, attenuation of PSF1 expression in HSCs may cause prolonged BM suppression after chemotherapy and pancytopenia with aging. So far, the association of stem cell division with DNA replication proteins in hematopoietic disorders has not been reported. It is intriguing to analyze the relationship of hematopoietic diseases and DNA replication protein, such as PSF1. Based on our analysis, identification of *PSF1*-dependent genes probably sheds light on the mechanism of DNA replication in HSCs and ontogeny of hematopoietic disorders.

Acknowledgments

We thank Dr T. Watanabe (Tohoku University, Japan) for providing us the *AML-1/Runx1* mutant mice, and Ms Y. Shimizu, Ms K. Ishida, Ms M. Sato, Mrs Y. Nakano, Mrs K. Fukuhara, and Mrs N. Fujimoto for technical assistance.

This work was supported in part by the Japanese Ministry of Education, Culture, Sports, Science and Technology and the Japan Society for Promotion of Science.

Authorship

Contribution: M.U. and N.T. designed the research, analyzed data, and wrote the paper; K.S. and M.A. helped generate PSF1 mutant mice; and M.I. helped generate anti-PSF1 antibody.

Conflict-of-interest disclosure: The authors declare no competing financial interests.

Correspondence: Nobuyuki Takakura, Department of Signal Transduction, Research Institute for Microbial Diseases, Osaka University, 3-1 Yamada-oka, Suita, Osaka 565-0871, Japan; e-mail: ntakaku@biken.osaka-u.ac.jp.

References

1. Cheshier SH, Morrison SJ, Liao X, Weissman IL. In vivo proliferation and cell cycle kinetics of long-term self-renewing hematopoietic stem cells. Proc Natl Acad Sci U S A. 1999;96:3120-3125.
2. Osawa M, Hanada K, Hamada H, Nakauchi H. Long-term lymphohematopoietic reconstitution by a single CD34-low/negative hematopoietic stem cell. Science. 1996;273:242-245.
3. Calvi LM, Adams GB, Weibrecht KW, et al. Osteoblastic cells regulate the haematopoietic stem cell niche. Nature. 2003;425:841-846.
4. Reya T, Duncan AW, Ailles L, et al. A role for Wnt signalling in self-renewal of haematopoietic stem cells. Nature. 2003;423:409-414.
5. Varnum-Finney B, Xu L, Brashem-Stein C, et al. Pluripotent, cytokine-dependent, hematopoietic stem cells are immortalized by constitutive Notch1 signaling. Nat Med. 2000;6:1278-1281.
6. Kanemaki M, Sanchez-Diaz A, Gambus A, Labib K. Functional proteomic identification of DNA replication proteins by induced proteolysis in vivo. Nature. 2003;423:720-724.
7. Kubota Y, Takase Y, Komori Y, et al. A novel ring-like complex of Xenopus proteins essential for the initiation of DNA replication. Genes Dev. 2003;17:1141-1152.
8. Takayama Y, Kamimura Y, Okawa M, Muramatsu S, Sugino A, Araki H. GINS, a novel multiprotein complex required for chromosomal DNA replication in budding yeast. Genes Dev. 2003;17:1153-1165.
9. De Falco M, Ferrari E, De Felice M, Rossi M, Hübscher U, Pisani FM. The human GINS complex binds to and specifically stimulates human DNA polymerase alpha-primase. EMBO Rep. 2007;8:99-103.
10. Kamada K, Kubota Y, Arata T, Shindo Y, Hanaoka F. Structure of the human GINS complex and its assembly and functional interface in replication initiation. Nat Struct Mol Biol. 2007;14:388-396.
11. Boskovic J, Coloma J, Aparicio T, et al. Molecular architecture of the human GINS complex. EMBO Rep. 2007;8:678-684.
12. Choi JM, Lim HS, Kim JJ, Song OK, Cho Y. Crystal structure of the human GINS complex. Genes Dev. 2007;21:1316-1321.
13. Chang YP, Wang G, Bermudez V, Hurwitz J, Chen XS. Crystal structure of the GINS complex and functional insights into its role in DNA replication. Proc Natl Acad Sci U S A. 2007;104:12685-12690.
14. Pacek M, Tutter AV, Kubota Y, Takisawa H, Walter JC. Localization of MCM2-7, Cdc45, and GINS to the site of DNA unwinding during eukaryotic DNA replication. Mol Cell. 2006;21:581-587.
15. Bauerschmidt C, Pollok S, Kremmer E, Nasheuer HP, Grosse F. Interactions of human Cdc45 with the Mcm2-7 complex, the GINS complex, and DNA polymerases delta and epsilon during S phase. Genes Cells. 2007;12:745-758.

16. Moyer SE, Lewis PW, Botchan MR. Isolation of the Cdc45/Mcm2-7/GINS (CMG) complex, a candidate for the eukaryotic DNA replication fork helicase. Proc Natl Acad Sci U S A. 2006;103:10236-10241.
17. Gambus A, Jones RC, Sanchez-Diaz A, et al. GINS maintains association of Cdc45 with MCM in replisome progression complexes at eukaryotic DNA replication forks. Nat Cell Biol. 2006;8:358-366.
18. Ueno M, Itoh M, Kong L, Sugihara K, Asano M, Takakura N. PSF1 is essential for early embryogenesis in mice. Mol Cell Biol. 2005;25:10528-10532.
19. Okada H, Watanabe T, Niki M, et al. AML1(−/−) embryos do not express certain hematopoiesis-related gene transcripts including those of the PU.1 gene. Oncogene. 1998;17:2287-2293.
20. Takakura N, Yoshida H, Ogura Y, Kataoka H, Nishikawa S, Nishikawa S. PDGFR alpha expression during mouse embryogenesis: immunolocalization analyzed by whole-mount immunohistostaining using the monoclonal anti-mouse PDGFR alpha antibody APA5. J Histochem Cytochem. 1997;45:883-893.
21. Takakura N, Huang XL, Naruse T, et al. Critical role of the TIE2 endothelial cell receptor in the development of definitive hematopoiesis. Immunity. 1998;9:677-686.
22. Takakura N, Watanabe T, Suenobu S, et al. A role for hematopoietic stem cells in promoting angiogenesis. Cell. 2000;102:199-209.
23. Kong L, Ueno M, Itoh M, Yoshioka K, Takakura N. Identification and characterization of mouse PSF1-binding protein, SLD5. Biochem Biophys Res Commun. 2006;339:1204-1207.
24. Nakauchi H, Takano H, Ema H, Osawa M. Further characterization of CD34-low/negative mouse hematopoietic stem cells. Ann NY Acad Sci. 1999;872:57-70.
25. Tajima F, Deguchi T, Laver JH, Zeng H, Ogawa M. Reciprocal expression of CD38 and CD34 by adult murine hematopoietic stem cells. Blood. 2001;97:2618-2624.
26. Morrison SJ, Hemmati HD, Wandycz AM, Weissman IL. The purification and characterization of fetal liver hematopoietic stem cells. Proc Natl Acad Sci U S A. 1995;92:10302-10306.
27. Okuda T, van Deursen J, Hiebert SW, Grosveld G, Downing JR. AML1, the target of multiple chromosomal translocations in human leukemia, is essential for normal fetal liver hematopoiesis. Cell. 1996;84:321-330.
28. Darnowski JW, Handschumacher RE. Tissue-specific enhancement of uridine utilization and 5-fluorouracil therapy in mice by benzylacyclouridine. Cancer Res. 1985;45:5364-5368.
29. Randall TD, Weissman IL. Phenotypic and functional changes induced at the clonal level in hematopoietic stem cells after 5-fluorouracil treatment. Blood. 1997;89:3596-3606.
30. Barker N, van Es JH, Kuipers J, et al. Identification of stem cells in small intestine and colon by marker gene Lgr5. Nature. 2007;449:1003-1007.
31. Akala OO, Clarke MF. Hematopoietic stem cell self-renewal. Curr Opin Genet Dev. 2006;16:496-501.
32. Lambert JF, Liu M, Colvin GA, et al. Marrow stem cells shift gene expression and engraftment phenotype with cell cycle transit. J Exp Med. 2003; 197:1563-1572.
33. Huang HK, Bailis JM, Leverson JD, Gómez EB, Forsburg SL, Hunter T. Suppressors of Bir1p (Survivin) identify roles for the chromosomal passenger protein Pic1p (INCENP) and the replication initiation factor Psf2p in chromosome segregation. Mol Cell Biol. 2005;25:9000-9015.
34. Ulrich CM, Robien K, McLeod HL. Cancer pharmacogenetics: polymorphisms, pathways and beyond. Nat Rev Cancer. 2003;3:912-920.

Theme Issue Article

Maturation of blood vessels by haematopoietic stem cells and progenitor cells: Involvement of apelin/APJ and angiopoietin/Tie2 interactions in vessel caliber size regulation

Nobuyuki Takakura; Hiroyasu Kidoya

Department of Signal Transduction, Research Institute for Microbial Diseases, Osaka University, Osaka, Japan

Summary

Apelin is a recently-isolated bioactive peptide from bovine gastric extract. The gene encodes a protein of 77 amino acids, which can generate two active polypeptides, long (42–77) and short (65–77). Both peptides ligate and activate APJ, a G protein-coupled receptor expressed in the cardiovascular and central nervous systems. Although an essential role for the apelin/APJ system in blood vessel formation has been reported in *Xenopus*, its precise function in mammals is unclear. Blood vessel tube formation is accomplished by two main mechanisms: 1) single cell hollowing, in which a lumen forms within the cytoplasm of a single endothelial cell (EC), and 2) cord hollowing in which a luminal cavity is created *de novo* between ECs in a thin cylindrical cord. Molecular control of either single cell or cord hollowing has not been precisely determined. Angiopoietin-1 (Ang1) has been reported to induce enlargement of blood vessels. Apelin is produced from ECs upon activation of Tie2, a cognate receptor of Ang1, expressed on ECs. It has been suggested that apelin induces cord hollowing by promoting proliferation and aggregation/assembly of ECs. During angiogenesis, haematopoietic stem cells (HSCs) and progenitor cells (HPCs) are frequently observed in the perivascular region. They produce Ang1 and induce migration of ECs, resulting in a fine vascular network. Moreover, HSCs/HPCs can induce apelin production from ECs. Therefore, this review article posits that HSCs/HPCs regulate caliber size of blood vessels via apelin/APJ and Angiopoietin/Tie2 interactions.

Keywords

Haematopoietic stem cell, haematopoietic progenitor cells, Tie2, Angiopoietin-1, Apelin, APJ

Thromb Haemost 2009; 101: 999–1005

Blood vessel size determination

The formation of blood vessels is initiated by the assembly of endothelial cells (ECs), or EC progenitors, and their subsequent tube formation. This process is termed vasculogenesis and is followed by angiogenesis, which results in the emergence of new vessels through the sprouting and elongation from, or the remodeling of, preexisting vessels (1). In both processes, to maintain the structural stability of nascent EC tubes, mural cells (MCs) such as smooth muscle cells and pericytes are recruited around the forming tube and adhere to ECs.

Many genes and molecules involved in these processes have been identified (2–10), with vascular endothelial growth factor (VEGF) mainly playing a role in the development and tube formation of ECs. The ECs forming the tube recruit supporting MCs by releasing PDGF-BB (11). MCs subsequently adhere to ECs resulting in the formation of a structurally stable blood vessel. It has been reported that this cell adhesion between ECs and MCs is induced when angiopoietin-1 (Ang1), produced by MCs, stimulates Tie2, a receptor tyrosine kinase on ECs (12–15). Therefore, Ang1 is involved in the maturation process of blood vessels. One of these maturation processes for blood vessel formation is adjustment of caliber size, which is very important to supply oxygen and nutrient adequately to tissues. Understanding the process of caliber size regulation is crucial for developing improved clinical approaches to treat cancer and hypoxic disease. However, the molecular mechanisms of blood vessel caliber size determination are not yet clearly understood.

Tube formation is a fundamental mechanism for organ and tissue generation in most major organs, such as the lung and kidney, as well as the vasculature. The molecular mechanisms involved in tube generation in general are not perfectly under-

Correspondence to:
Prof. Nobuyuki Takakura
Department of Signal Transduction, Research Institute for Microbial Diseases
Osaka University
3-1 Yamadaoka, Suita-shi, Osaka 565-0871, Japan
Tel.: +81 6 6879 8316, Fax: +81 6 6879 8314
E-mail: ntakaku@biken.osaka-u.ac.jp

Financial support:
This work was partly supported by the Japanese Ministry of Education, Culture, Sports, Science and technology.

Received: June 9, 2008
Accepted after minor revision: July 26, 2008

Prepublished online: January 15, 2009
doi:10.1160/TH08-06-0358

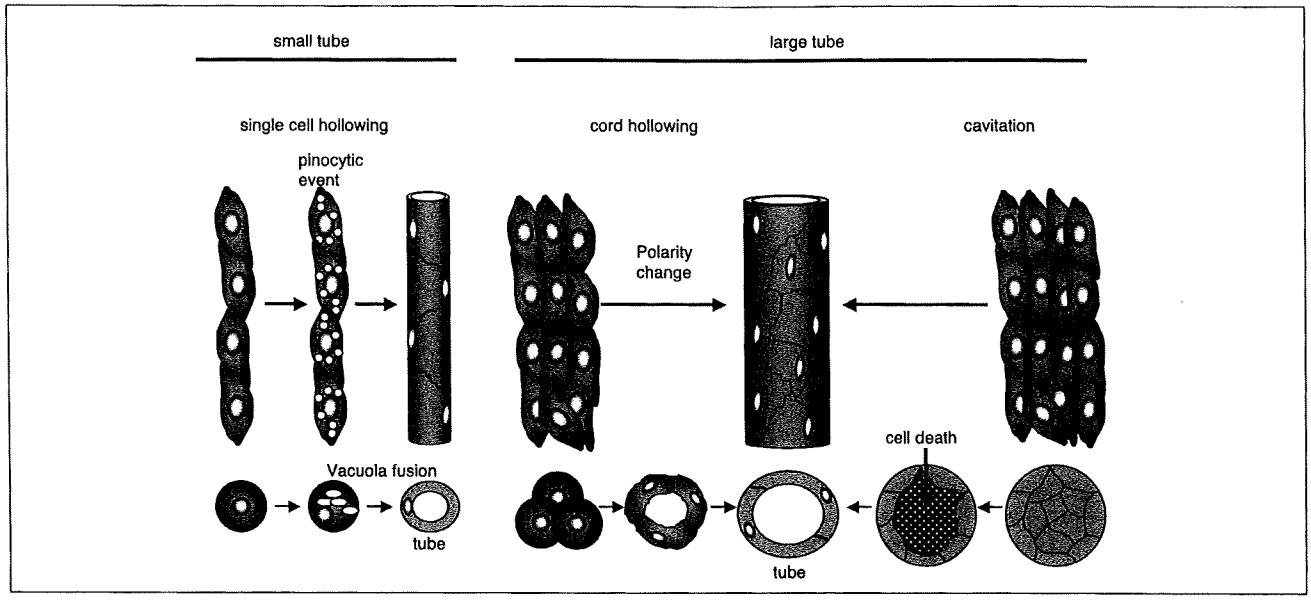

Figure 1: Tube formation in the vascular system. Schematic representation of tube formation observed in the vascular system. In single-cell hollowing, several vacuoles generated in the cytoplasm of an endothelial cell (EC) fuse with each other by pinocytic events, forming a tube within the cell. This then connects with the tube in an adjacent EC, resulting in formation of a narrow capillary tube. On the other hand, aggregated ECs change their polarity into either apical or basal orientation and gradually form tubes, resulting in the generation of enlarged blood vessels (cord hollowing). When ECs in the center of the aggregate are eliminated by apoptosis or differentiation into another lineage (i.e. haematopoietic cells), a tube will be formed (cavitation).

stood; however, anatomical observations of tube morphogenesis by epithelial cells have been well-described and show that tube development can occur in many different ways (16). Based on previous observations of tube formation in general, tubes in the vasculature might be generated by the following steps (Fig. 1). 1) single-cell hollowing: a lumen forms within the cytoplasm of a single EC; 2) cord hollowing: a luminal cavity is created *de novo* between ECs in a thin cylindrical cord; 3) cavitation: the central cells of a column composed of assembled ECs or endothelial progenitors are eliminated, forming a luminal cavity (this process may be less likely in angiogenesis, but has been observed in blood islands of the yolk sac); and 4) Wrapping or intussusception: an EC sheet invaginates and curls until the edges of the invaginating region meet and seal.

Recently, Kamei et al. (17) clearly demonstrated activity of the single-cell hollowing system for blood vessel formation in Zebrafish. Their in-vivo imaging technique showed that intracellular and intercellular fusion of endothelial vacuoles drives vascular lumen formation. Folkman and Haudenschild (18) described „longitudinal vacuoles" that „appeared to be extruded and connected from one cell to the next" in EC culture experiments *in vitro*. Therefore, single-cell hollowing may be able to construct capillaries of narrow caliber. However, the size of a single EC is limited, so single-cell hollowing cannot give rise to larger vessels. Thus, the cord hollowing system is required for constructing larger vessels. Identification of molecules utilised in cord hollowing but not in single-cell hollowing would therefore lead to a better understanding of how blood vessel caliber size is determined.

For cord hollowing, ECs once assembled and aggregated gradually manifest polarity, with luminal and apical regions. In-vivo experiments using zebrafish showed that the EC-derived secreted factor Egfl7 had a crucial role in proper lumen formation after aggregation of endothelial progenitors by regulating their polarity (19). Although the mechanism by which Egfl7 regulates lumen size has not yet been elucidated because of the difficulty of isolating its receptor, these findings imply that tube formation by single-cell hollowing does not occur in areas where ECs need to generate larger tubes.

Depending on the degree of tissue demand for oxygen, one EC starts to sprout from pre-existing vessels for the generation of small-sized capillaries by single-cell hollowing, but under severe hypoxia, several ECs assemble in one sprouting point from pre-existing vessels and generate larger vessels by a cord hollowing mechanism. Therefore, in the initiation of cord hollowing, several ECs/EC progenitors are required. Thus, for cord hollowing, on sensing hypoxia, ECs need to proliferate and assemble to constitute large cylinders, whereas for single-cell hollowing, proliferation is not required (Fig. 1).

Tie2 activation induces apelin in ECs

The Angl/Tie2 and VEGF/VEGFR systems are potent regulators influencing caliber size determination in blood vessels. Transgenic overexpression of Angl in keratinocytes induces enlarged blood vessel formation in the dermis (20) and administration of a potent Angl variant was also reported to result in enlargement of blood vessels (21, 22). Therefore, knowledge of the precise molecular mechanism of Angl/Tie2 induction of blood